Altered *hsrω* lncRNA levels in activated Ras background further enhance Ras activity in *Drosophila* eye and induces more R7 photoreceptors

Mukulika Ray and Subhash C. Lakhotia*

Cytogenetics Laboratory, Department of Zoology, Banaras Hindu University, Varanasi 221005

*** Corresponding author**

email: lakhotia@bhu.ac.in

ORCID ID:

Mukulika Ray: 0000-0002-9064-818X

S. C. Lakhotia: 0000-0003-1842-8411

Running Title: *hsrω* lncRNA & Ras activity in fly eyes

Keywords: Yan, Raf, p-MAPK, Ras-signaling

Abstract

We examined roles of *hsrω* lncRNAs in Ras signaling by down- or up-regulating them in *sev-GAL4* driven activated Ras^{V12} expressing *Drosophila* eye discs. Late pupal lethality and extra R7 photoreceptors in ommatidia caused by *sev-GAL4>*Ras^{V12} expression were significantly enhanced following simultaneous down- or up-regulation of *hsrω* lncRNAs. Ras signaling increased cell autonomously as well as non-autonomously, as revealed by enhanced p-MAPK expression, reduced Yan levels, greater RafRBDFLAG associated Ras and more R7 rhabdomeres. The further enhanced elevated Ras signaling seems to be due to post-transcriptional modifications in activities of Ras and its down-stream signaling members because of the disrupted intra-cellular dynamicity of many omega speckle associated hnRNPs and other RNA-binding proteins following down- or up-regulation of *hsrω* lncRNAs in elevated active Ras background. Co-altered *hsrω* RNA levels also modulated expression of certain sn/sno/scaRNAs and some other RNA processing genes affected in *sev-GAL4>*Ras^{V12}discs. Down-regulation of *hsrω* transcripts in such background elevated positive modulators of Ras signaling while *hsrω* up-regulation reduced negative-modulators, further enhancing Ras signaling in either condition. Cell autonomous and non-autonomous enhancement of hyperactive Ras by lncRNAs has implications for cell signaling during normal and high Ras activity, commonly associated with some cancers.

Summary

Our findings highlight roles of *hsrω* lncRNAs in conditionally modulating the important Ras signaling pathway and provide evidence for cell non-autonomous Ras signaling in *Drosophila* eye discs.

Introduction

Evolution of multi-cellularity and the associated division of labour has necessitated inter-cellular signaling pathways with complex regulatory circuits. Evolution of biological complexity is also paralleled by substantial increase in the non-coding component in diverse genomes, and there is increasing realization in recent years that the diverse short and long non-coding RNAs (lncRNA) have great roles in cell signaling and gene regulation (Geisler and Coller, 2013; Huang et al., 2013; Jose, 2015; Lakhotia, 2016; Lakhotia, 2017a; Lakhotia, 2017b; Mattick and Makunin, 2006; Morris and Mattick, 2014; Peng et al., 2017). Besides their roles in developmental regulation (Katsushima et al., 2016; Kotake et al., 2016; Lakhotia, 2017b; Misawa et al., 2017; Zhang et al., 2017a), diverse lncRNAs interact with signaling pathways in cancer to cause proliferation or apoptosis (Lakhotia, 2016; Liu et al., 2015; Wang et al., 2015).

The RAS/RAF/MAPK signaling pathway regulates many developmental processes with roles also in many human cancers (Fernández-Medarde and Santos, 2011; Pylayeva-Gupta et al., 2011). Ectopic expression of activated Ras causes hyperplastic growth in *Drosophila* also (Karim and Rubin, 1998; Prober and Edgar, 2000). An earlier study (Ray and Lakhotia, 1998) showed mutant alleles of *ras* (*ras*^{E62K} and *ras*^{D38N}) to dominantly enhance the embryonic lethality due to nullisomy of *hsrω* gene, which produces multiple lncRNAs (Lakhotia, 2011; Lakhotia, 2017a).

This study further examines interaction between altered levels of *hsrω* lncRNAs and ectopically expressed activated Ras producing *UAS-Ras*^{V12} transgene in developing eye discs. The *sev-GAL4* driven expression of *Ras*^{V12} increases R7 photoreceptors leading to ommatidial derangement and rough eyes (Karim et al., 1996). Intriguingly, reduced or enhanced levels of *hsrω* lncRNAs in *sev-GAL4>Ras*^{V12} expressing discs substantially enhanced activated Ras in cell autonomous as well as non-autonomous manner resulting in further increase in R7 photoreceptor number. Transcriptome analysis of eye discs with down- or up-regulated *hsrω* transcripts in normal Ras or *sev-GAL4*>activated Ras expression backgrounds and those expressing *sev-GAL4*>activated Ras in normal *hsrω* background revealed that either down- or up-regulation of *hsrω* lncRNAs in normal Ras background resulted in many similar, but hardly any opposite, transcriptomic changes. Analysis of expression of transcription factor (TF) and RNA binding protein (RBP) genes revealed similar or unique, but not opposite effects of down- or up-regulation of *hsrω* lncRNAs. Transcription of the major members of Ras/Raf/MAPK pathway was not significantly affected by altered *hsrω* RNA levels in normal or elevated activated Ras background. Interestingly, while down-regulation of *hsrω* activity in activated Ras background up-regulated some positive modulators of Ras signaling, up-regulation of these transcripts down-regulated several negative regulators of Ras/Raf/MAPK pathway, resulting in enhanced Ras activity in either situations. Over- or under-expression of the *hsrω* nuclear lncRNAs affects dynamics of the omega speckle associated RNA binding proteins (RBP), including diverse hnRNPs (Lakhotia et al., 2012; Piccolo et al., 2018; Piccolo and Yamaguchi, 2017; Prasanth et al., 2000; Singh and

Lakhotia, 2015), some of which have potential binding sites on transcripts of Ras signaling modulators.

The present study shows that altered levels of lncRNAs, like those produced by *hsrω*, can further enhance ectopically elevated Ras-signaling not only in same cells but also non-autonomously in neighboring cells. These findings thus have implications for modulation of Ras signaling in disease conditions like cancer by lncRNAs. Our initial results were placed at pre-print archive (Ray and Lakhotia, 2017).

Results

Down- as well as up-regulation of *hsrω* RNA levels aggravates phenotypes due to *sev-GAL4* driven expression of activated Ras in eye discs

We used *sev-GAL4>UAS-Ras*^{V12} expression, which leads to additional R7 rhabdomeres and rough eyes because the active Ras product triggers Ras signaling even in absence of upstream receptor tyrosine kinase (RTK) activation (Karim et al., 1996). Levels of the >10kb long nuclear lncRNAs produced by *hsrω* gene were down regulated through expression of *UAS-hsrωRNAi* transgene (Mallik and Lakhotia, 2009) and up-regulated by using the GAL4 inducible *EP3037* (Liao et al., 2000; Mallik and Lakhotia, 2009) allele. We also used the *UAS-pUHEx2A* RNAi transgenic line (R. Sahu and S. C. Lakhotia, unpublished) against *hsrω* gene's exon 2, and the *EP93D* over-expression allele of *hsrω* (Mallik and Lakhotia, 2009).

At 24±1°C, only ~12% (N =1058) *sev-GAL4> Ras*^{V12} pupae emerged as adults displaying rough eyes with de-pigmented patches and occasional black spots (Fig 1A) while ~88% died as pharates (Fig 1B). Following co-expression of either *hsrωRNAi* (N = 1177) or *EP3037* (N = 1109) in *sev-GAL4* driven *Ras*^{V12} background, majority died as early pupae and the rest as late pupae (Fig. 1A, B), indicating enhanced effects on ectopic activated Ras expression. As reported earlier (Mallik and Lakhotia, 2011), *sev-GAL4* driven expression of *UAS-hsrωRNAi* or *EP3037* in normal wild type Ras background did not cause any eye phenotype (not shown). To examine adult eye phenotypes, these three genotypes were reared at 18±1°C to weaken the GAL4 driven expression (Brand et al., 1994; Mondal et al., 2007). At 18±1°C, more than 80% flies (N= ~ 1000 flies for each genotype) eclosed in each case, with no early pupal lethality (Fig. 1C). At 18°C too, the *sev-GAL4* driven activated Ras expression caused roughening of eyes in all adults (Fig. 1E, I) which was enhanced when *sev-GAL4* driven *hsrωRNAi* or *EP3037* and *Ras*^{V12} were co-expressed (Fig. 1C-D, J-H).

When *sev-GAL4>UAS-pUHEx2A* was co-expressed with activated Ras at 24±1°C, early pupal death, similar to that with *UAS-hsrωRNAi*, was observed (not shown). Similarly, over expression of *hsrω* lncRNAs with *sev-GAL4>EP93D* resulted in pupal lethality (not shown) similar to that in *sev-GAL4>Ras*^{V12} *EP3037* genotype.

In view of similar results with two different *hsrωRNAi* transgenes and two different *EP* alleles we used the *UAS-hsrωRNAi* and *EP3037* in subsequent studies.

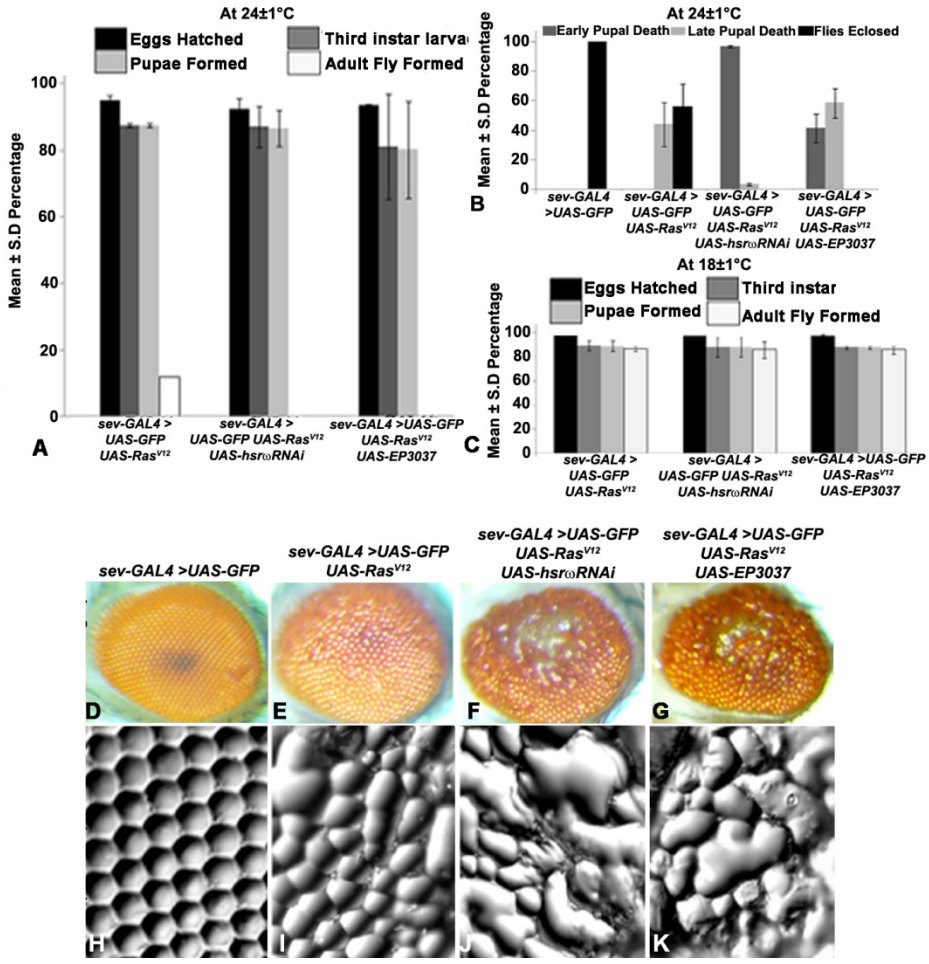

Fig. 1. Alterations in *hsrω* RNAs levels enhance pupal lethality and roughening of eyes due to *sev-GAL4* driven activated Ras expression. A Mean percent (± S.D.) survival (Y-axis) of different genotypes (X-axis) till different stages of development. **B** mean percent lethality of pupae reared and flies eclosed at 24±1°C. **C** mean percent (± S.D.) survival (Y-axis) of different genotypes (X-axis) till different stages of development when reared at 18±1°C. **D-G** Photomicrographs and **H-K** nail polish imprints of adult eyes in different genotypes (noted above each column) reared at 18±1°C.

The photoreceptor and *sev-GAL4>UAS-GFP* expressing cells in mature ommatidia from the posterior most region in different genotypes were counted after Elav immunostaining (Fig. 2A-D). Because of high derangement and fusion of ommatidia in *sev-GAL4>UAS-Ras^{V12} UAS-hsrωRNAi* and *sev-GAL4>UAS-Ras^{V12} EP3037* genotypes, fewer individual ommatidia could be unambiguously examined in these genotypes. Examination of eye discs of *sev-GAL4> UAS-*

Ras^{V12}, *sev-GAL4>Ras*^{V12} *UAS-hsrωRNAi* and *sev-GAL4> UAS-Ras*^{V12} *EP3037* genotypes revealed that Elav+ve cells were increased in *sev-GAL4>UAS-Ras*^{V12} and further increased when *hsrω* transcripts were co-altered (compare Fig 2A-B with Fig 2C-D). In agreement with known expression of *sev-GAL4* driver (Ray and Lakhotia, 2015), a subset of Elav+ve photoreceptors, and the future cone cells were GFP+ve. Data in Supplementary Table S1 show that numbers of GFP+ve/Elav-ve (cone cells) and GFP-ve/Elav+ve (photoreceptors not expressing *sev-GAL4*) remained unchanged in all genotypes but those of GFP+ve and Elav+ve (sevenless lineage photoreceptors) increased in *sev-GAL4>UAS-Ras*^{V12} discs, still more in *sev-GAL4>UAS-Ras*^{V12} *EP3037* discs and were maximum in *sev-GAL4>UAS-Ras*^{V12} *UAS-hsrωRNAi* eye discs (Fig. 2A-D, Supplementary Table S1)

The additional photoreceptors in eye discs with altered of *hsrω* transcript levels in activated Ras expression background are R7 type

The Ras/Raf/MAPK signaling dependent differentiation of the multiple R7 precursor cells in normal development into the definitive R7 photoreceptor is initiated by binding of Boss ligand to the Sevenless RTK and activation of Ras (Mavromatakis and Tomlinson, 2016; Tomlinson and Struhl, 2001), which initiates signaling cascade culminating in phosphorylation and nuclear translocation of MAPK to trigger the downstream events for R7 differentiation (Karin and Hunter, 1995). Since the Ras^{V12} does not need ligand binding for activation, the *sev-GAL4>UAS-Ras*^{V12} expression directly drives differentiation of two or more R7 photoreceptor cells per ommatidium.

We used Runt antibody to confirm that the additional GFP+ve and Elav+ve photoreceptor cells in the experimental genotypes indeed belonged to the R7 lineage (Edwards and Meinertzhagen, 2009; Tomlinson et al., 2011). Runt identified R7 and R8 but R7 was differentiated from R8 because of *sev-GAL4>UAS-GFP* expression and its location in a different tissue plane. In wild type (*sev-GAL4>UAS-GFP*) discs, R7 cells formed a defined pattern with only one Runt and GFP-positive rhabdomere in each ommatidium (Fig 2E). Runt and GFP+ve rhabdomeres increased in *sev-GAL4>UAS-Ras*^{V12}, *sev-GAL4>UAS-Ras*^{V12} *EP3037* and *sev-GAL4>UAS-Ras*^{V12} *UAS-hsrωRNAi* discs and consequent disorganization of ommatidial arrays in that order (Fig. 2E-H, Supplementary Table S1). Elav and Runt staining together thus show that the increase in number of rhabdomeres per ommatidium in *sev-GAL4>UAS-Ras*^{V12}, *sev-GAL4>UAS-Ras*^{V12} *EP3037* and *sev-GAL4>UAS-Ras*^{V12} *UAS-hsrωRNAi* is essentially due to increasingly more R7 cells.

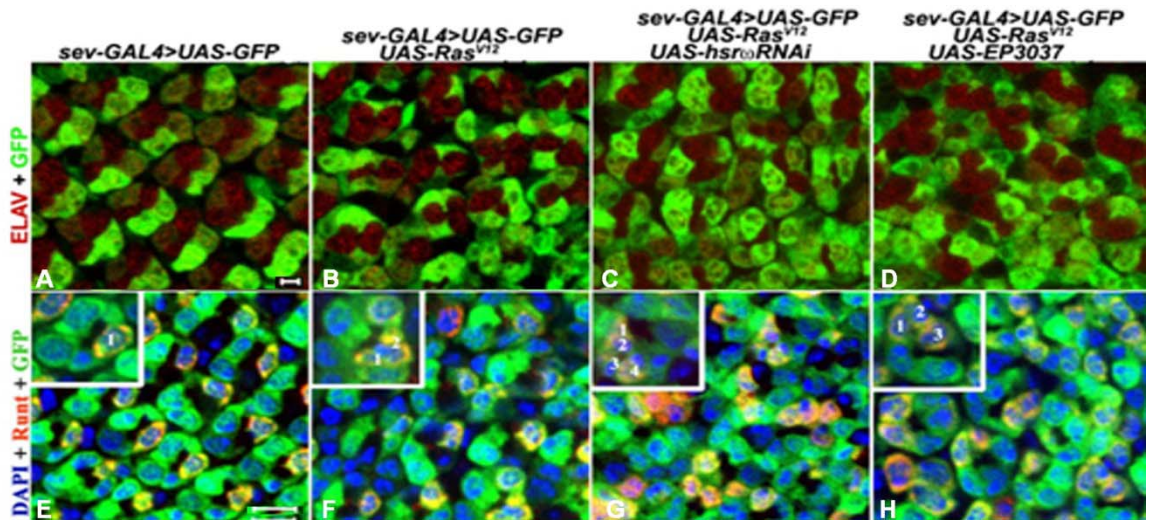

Fig. 2. Altered *hsrω* RNA levels in activated Ras expression background promote more cells to R7 photoreceptor fate. A-H Confocal optical sections of eye discs of different genotypes (noted above each column) showing Elav stained photoreceptors (red, **A-D**) and Runt positive R7 photoreceptors (red, **E-H**); the *sev-GAL4>GFP* expressing cells are green in **A-H**; counterstaining with DAPI (blue, **E-H**). Insets in **E-H** show single representative ommatidium, with the Runt and GFP+ve cells numbered. Scale bar = 2µm in **A** and 5µm in **E** and applies to **A-D** and **E-H**, respectively

Altered *hsrω* RNA levels further enhance Ras signaling in cell autonomous as well as non-autonomous manner in eye discs expressing *sev-GAL4* driven activated Ras

Presence of more R7 photoreceptors in eye discs with altered levels of *hsrω* transcripts in activated Ras expression background suggested further increase in Ras signaling. Therefore, we examined p-MAPK distribution since MAPK phosphorylation and its nuclear translocation measures active Ras signaling (Karin and Hunter, 1995). We also examined levels of Yan, a transcription factor (TF) negatively regulated by Ras signaling (Brunner et al., 1994; O'Neill et al., 1994).

In *sev-GAL4>UAS-GFP* eye discs, only a few cells per ommatidium showed nuclear p-MAPK (Fig 3A, M). Expression of activated Ras led more cells to show nuclear p-MAPK (Fig 3B, M) with an overall increase in p-MAPK presence. When *hsrω* RNA levels were concomitantly down- (Fig 3C) or up-regulated (Fig 3D), the number of cells with nuclear p-MAPK increased steeply (Fig 3C-D, M) with similar rise in overall p-MAPK levels. Interestingly, not only the GFP+ve cells, but non *sev-GAL4* expressing GFP-negative cells (arrows in Fig 3B-D) also showed higher p-MAPK levels, suggesting a non-autonomous Ras signaling.

Yan is very highly expressed in the morphogenetic furrow (MF) (arrows in Fig 3E-H) but its staining progressively declined from anterior to posterior region, with weakest presence in posterior-most differentiated photoreceptors. Following *sev-GAL4* driven expression of activated

Ras, a small but perceptible decrease in Yan expression occurred along the antero-posterior axis and at the MF (Fig 3F). Either down- or up-regulation of *hsrω* RNA in the *sev-GAL4* driven activated Ras expression background further reduced Yan (Fig 3G-H), including in the MF cells. Since the *sev-GAL4* driver has no expression at the MF (Ray and Lakhotia, 2015), the distinct reduction in Yan staining all over the eye disc, including the MF, clearly indicates a cell non-autonomous Ras signaling.

To ascertain if the above changes in test genotypes were due to enhanced Ras expression and/or with a higher proportion of Ras being in an active form, we co-immunostained developing eye discs for Ras and RafRBDFLAG since the FLAG-tagged active Ras binding domain of Raf produced by the *UAS-RafRDBFLAG* construct (Freeman et al., 2010) binds only with active Ras (Fig. 3I-O). Little co-localization of the RafRBDFLAG with the native Ras was seen (Fig 3I) in *sev-GAL4* driven *UAS-RafRBDFLAG* expressing eye discs, which have normal developmental Ras expression. In contrast, FLAG tagged RafRBD and Ras substantially co-localized in eye discs expressing *sev-GAL4>UAS-Ras*^{V12}, as expected because active Ras expression (Fig 3J). Down- or up-regulation of *hsrω* RNAs in this background clearly enhanced the number of cells showing co-localized RafRBDFLAG and Ras (Fig 3K, L). Interestingly, a greater number of GFP-ve cells (Fig 3J-L), adjoining the GFP+ve cells, also showed colocalized Ras and RafRBDFLAG in discs co-expressing *sev-GAL4>UAS-Ras*^{V12} and *UAS-hsrωRNAi* or *EP3037*. Since neither RafRBDFLAG nor *UAS-Ras*^{V12} was expressed in the GFP-ve cells, their co-localization in such cells suggests movement of activated Ras complex from *sev-GAL4* expressing cells to the neighbors.

To know if the increased colocalization in more cells in eye discs expressing activated Ras, without or with altered *hsrω* RNA levels, reflected equal or differential elevation in total Ras, activated Ras and RafRBDFLAG protein levels, we quantified the Ras, FLAG, DAPI and GFP fluorescence using the histo option of Zeiss Meta 510 Zen software. Maximum projection images of 13 optical sections of each eye disc, which showed Elav positive photoreceptor cells, were used for this purpose. As seen in Fig. 3N, the total Ras was expectedly higher in *sev-GAL4>UAS-Ras*^{V12} than in *sev-GAL4>UAS-GFP* eye discs. More than 2 times further increase in Ras staining in discs co-expressing *UAS-hsrωRNAi* or *EP3037* with *UAS-Ras*^{V12} clearly shows further enhanced Ras levels following under- or over-expression of *hsrω* transcripts in activated Ras over-expression background. The increase in GFP staining in *sev-GAL4>UAS-Ras*^{V12} *UAS-hsrωRNAi* correlates with the above noted greater increase in *sev-GAL4* driven GFP expressing cells. The more or less comparable levels of DAPI fluorescence in samples of eyes discs in different genotypes indicates that the increase in Ras or GFP activity in specific genotypes is not due to a general increase in number of cells in some genotypes. Significantly, the levels of RafRBDFLAG protein showed the expected increase in *sev-GAL4>UAS-Ras*^{V12} over that in *sev-GAL4>UAS-GFP* eye discs but co-expression of *UAS-hsrωRNAi* or *EP3037* with activated Ras was not associated with further increase in the FLAG staining (Fig. 3N).

We examined colocalization of Ras and RafRBDFLAG fluorescence signals to determine how much of the enhanced levels of Ras in *sev-GAL4>UAS-Ras*^{V12} and more so in *sev-GAL4>UAS-Ras*^{V12} *UAS-hsrωRNAi* and *sev-GAL4>UAS-Ras*^{V12} *EP3037* eye discs was in activated form, (Fig. 3O), using the same sets of the maximum projection images of eye discs used for quantification of Ras and RafRBDFLAG (Fig. 3N). The co-localization option of the Zeiss Meta 510 Zen software was used following the Zeiss manual (https://www.zeiss.com/content/dam/Microscopy/Downloads/Pdf/FAQs/zenaim_colocalization.pdf). In agreement with the ectopic expression of activated Ras in *sev-GAL4>UAS-Ras*^{V12} eye discs, nearly 40% of RafRBDFLAG was associated with Ras compared to only about 5% in *sev-GAL4>UAS-GFP* discs. Interestingly, co-expression of *UAS-hsrωRNAi* or *EP3037* in *sev-GAL4>UAS-Ras*^{V12} eye discs further increased the association of Ras and RafRBDFLAG proteins (Fig. 3O), indicating greater proportion of Ras being in activated form with which the RafRBDFLAG can bind.

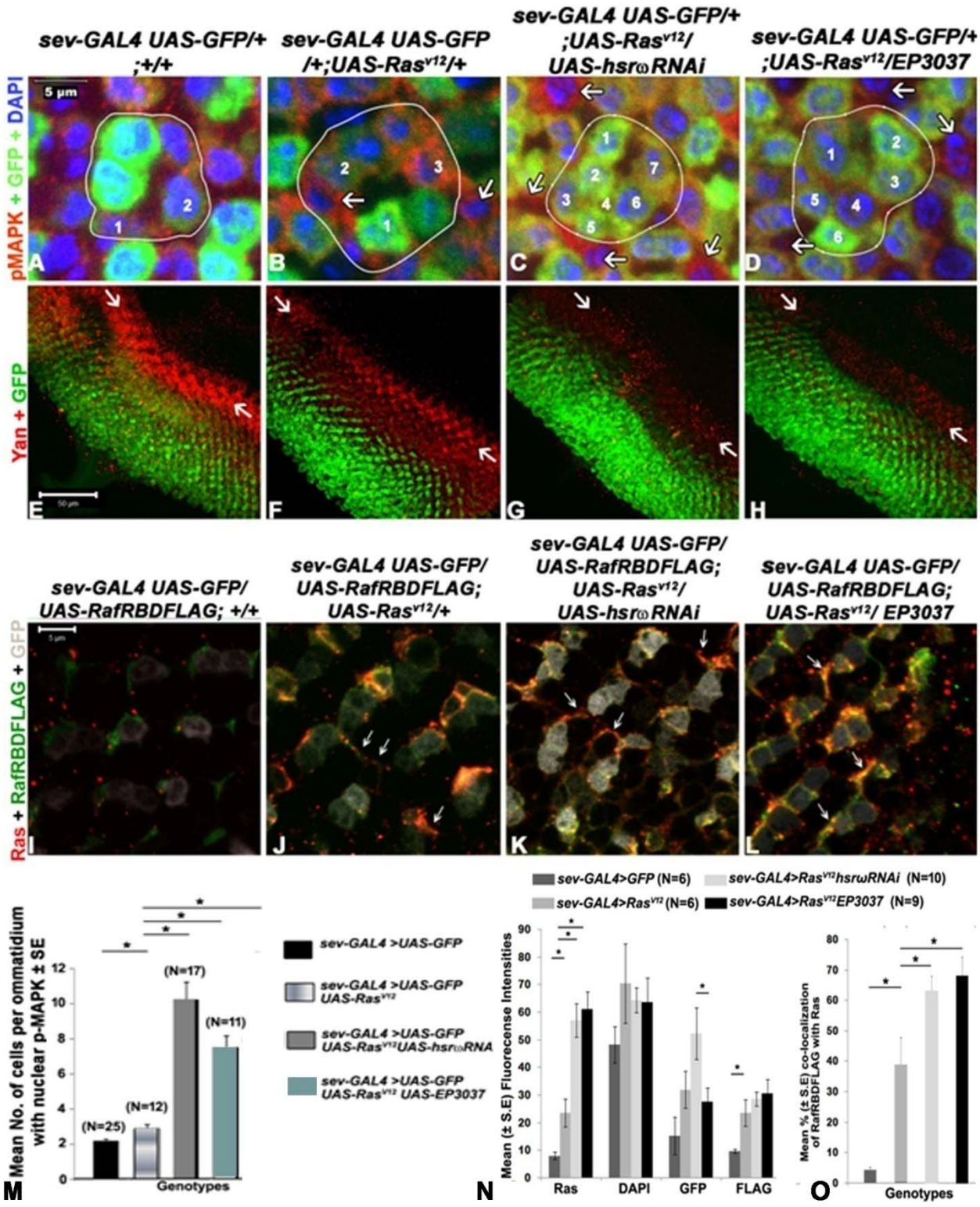

Fig. 3. Alterations in *hsrω* RNA levels in activated Ras expression background increases cell autonomous as well as non- autonomous Ras signaling. A-D Optical sections of parts of eye discs of different genotypes (noted above each column) showing p-MAPK immunostaining

(red) and *sev-GAL4* driven GFP (green, counterstained with DAPI, blue); a representative ommatidium in each is demarcated by white line with the rhabdomeres showing nuclear p-MAPK numbered. White arrows indicate some non-GFP expressing but p-MAPK +ve cells in **B-D**. Scale bar in **A** denotes 5µm and applies to **A-D. E-H** Optical sections of eye discs of different genotypes (noted above each column) showing Yan immunostaining (red) and *sev-GAL4* driven GFP (green). White arrows mark the Morphogenetic furrow. Scale bar in **E** denotes 50µm and applies to **E-H. I-L** Optical sections of parts of eye discs of different genotypes (noted above each column) showing Ras (red) and FLAG (green) immunostaining and *sev-GAL4>GFP* (grey). Scale bar in **I** denotes 5µm and applies to **I-L. M** Mean numbers of cells with nuclear p-MAPK per ommatidium in different genotypes (X-axis) identified in the key on right. The numbers of ommatidia examined for data in **M** are noted above each bar. **N** Mean intensities (Y-axis) of Ras, DAPI, GFP and RafRBDFLAG fluorescence (X-axis) in eye discs of different genotypes (key above). **O** Colocalization of RafRBDFLAG and Ras, expressed as mean percent (± S.E) of RafRBDFLAG protein associated with Ras in different genotypes. Number of eye discs observed (N) for each genotype is in the key above **N** and **O** panels. A horizontal line connecting specific pairs of bars and the * mark indicate significant differences ($P \leq 0.05$) between given pairs of means on Student's *t*-test.

To check if the above noted increase in Ras and activated Ras levels was associated with increased transcription of the resident *Ras* and/or *UAS-Ras^{V12}* transgene, levels of Ras transcripts derived from these two sources were examined using semi-quantitative RT-PCR with primers designed to differentiate between these two transcripts. The normal resident *Ras* transcripts remained more or less comparable in all the four genotypes (*sev-GAL4>UAS-GFP*, *sev-GAL4>UAS-Ras^{V12}*, *sev-GAL4>UAS-Ras^{V12} hsrωRNAi* and *sev-GAL4>UAS-Ras^{V12} EP3037*) and likewise, the transcripts derived from the *Ras^{V12}* transgene remained similar in *sev-GAL4>UAS-Ras^{V12}* and those co-expressing *hsrωRNAi* or *EP3037* with *UAS-Ras^{V12}* (Supplementary Fig S1 A and B). This indicated that the elevated Ras activity in the latter two genotypes with altered *hsrω* RNA levels is not due to increased transcription of *UAS-Ras^{V12}* transgene or the resident *Ras* gene. As noted later, the RNA-seq data also did not show any significant increase in Ras transcripts in *sev-GAL4>UAS-Ras^{V12}* eye discs co-expressing *hsrωRNAi* or *EP3037* compared to those expressing only activated Ras.

The *sev-GAL4* driven increase or decrease in *hsrω* lncRNA levels in normal Ras background had largely similar effects on the transcriptome of third instar larval eye discs

We sequenced total RNAs from *sev-GAL4>hsrωRNAi*, *sev-GAL4>EP3037*, *sev-GALl4>UAS-Ras^{V12}*, *sev-GAL4>UAS-Ras^{V12} hsrωRNAi* and *sev-GAL4>UAS-Ras^{V12} EP3037* eye discs to understand the underlying reasons for the unexpected common effect of down- or up-regulation of *hsrω* transcripts in elevated active Ras background.

RNA-seq data revealed that a large proportion of transcripts were indeed similarly affected by down- or up-regulation of *hsrω* RNA in normal Ras expression background; very few showed

opposing changes (Fig. 4; Supplementary Table S4, Sheets 1 and 2). Comparison of transcriptomes of *sev-GAL4>hsrωRNAi* and *sev-GAL4>EP3037* eye discs revealed that in each case more genes were down-regulated (Fig. 4A and B) than up-regulated. Compared to 319 commonly down-regulated (Fig. 4A) and 15 commonly up-regulated (Fig. 4B) genes in the two genotypes, only 2 showed opposing trends between *sev-GAL4>UAS-hsrωRNAi* and *sev-GAL4>EP3037* eye discs (Fig 4 C-D). While a detailed analysis of the transcriptomic changes in these two genotypes would be considered elsewhere, a brief analysis of the commonly affected genes that appear to be relevant in the present context is considered here.

Gene Ontology (GO) analysis of the 319 commonly down regulated genes in *sev-GAL4>hsrωRNAi* and *sev-GAL4>EP3037* eye discs identified several R7 photoreceptor differentiation and Ras signaling cascade genes. Many Ras signaling regulation genes were part of Ras/Rho signaling pathway (*Rhogef64c*, *CG43658, CG5937, dab*) while others were negative regulators of Ras signaling (*Nfat* and *Klu*). The R7 differentiation pathway genes (*drk*, *sos*) act upstream of Ras protein but downstream of receptor tyrosine kinase (Olivier et al., 1993). Since as noted earlier, R7 differentiation was not affected in these two genotypes, these transcriptomic changes apparently may not significantly alter the Ras/MAPK signaling and R7 differentiation.

We also checked status of known TF (Rhee et al., 2014) and RBP (RNA binding protein Database at http://rbpdb.ccbr.utoronto.ca) in *Drosophila melanogaster* as *hsrω* transcripts bind with diverse RBP that regulate gene expression and RNA processing (Lakhotia et al., 2012; Piccolo et al., 2018; Piccolo and Yamaguchi, 2017; Prasanth et al., 2000; Singh and Lakhotia, 2015). Of the nearly 1000 known TF (Rhee et al., 2014), 91 were commonly down-regulated following down- or up-regulation of *hsrω* transcripts (Fig. 4E) while 4 and 74 were uniquely down regulated in *sev-GAL4>UAS-hsrωRNAi* and *sev-GAL4>EP3037* eye discs, respectively (Fig. 4E). Among the 259 known RBP, 14 were commonly down regulated in both genotypes, while 16 were significantly down regulated only in *sev-GAL4>UAS-EP3037* eye discs and 2 only in *sev-GAL4>UAS-hsrωRNAi* (Fig. 4F). Interestingly, as shown later (Fig. 8A), all of the 16 RBP, which showed significant down regulation in *sev-GAL4>UAS-EP3037*, also showed a downward trend in *sev-GAL4>UAS-hsrωRNAi* eye discs. These 16 RBPs included some of the *hsrω* lncRNAs interactors like Hrb87F, Caz/dFus, TDP-43 (dTBPH) (Lakhotia et al., 2012; Piccolo et al., 2018; Piccolo and Yamaguchi, 2017; Prasanth et al., 2000; Singh and Lakhotia, 2015). Surprisingly, none of the examined RBPs were up-regulated when *hsrω* transcripts were altered.

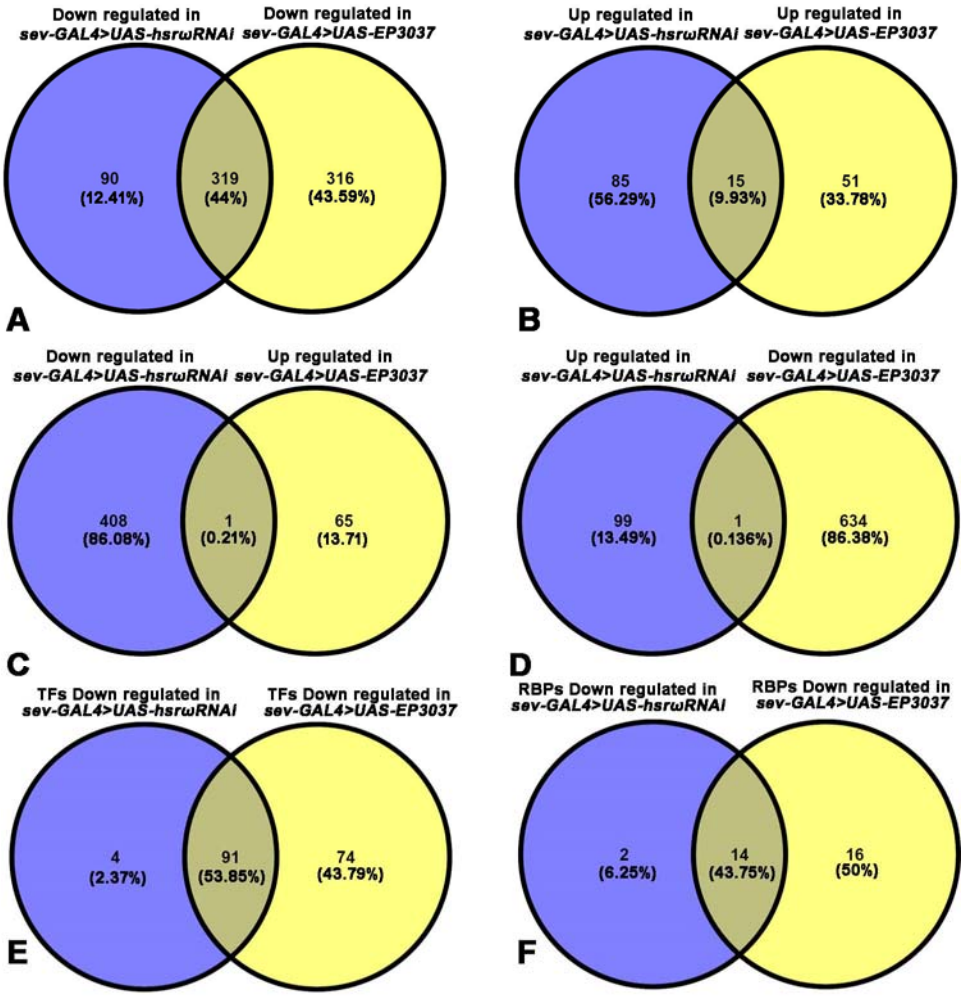

Fig. 4. The *sev-GAL4* driven down-or up-regulation of *hsrω* RNA in normal Ras expression background causes many common transcriptomic changes. A-B Venn diagrams showing numbers of genes down- (**A**) or up-regulated (**B**) in third instar *sev-GAL4>UAS-hsrωRNAi* or *sev-GAL4>EP3037* eye discs when compared with *sev-GAL4>UAS-GFP* control eye discs. **C-D** Venn diagrams showing numbers of genes down-regulated in *sev-GAL4>UAS-hsrωRNAi* but up-regulated in *sev-GAL4>UAS-EP3037* eye discs (**C**) and vise-versa (**D**). **E-F** Venn diagrams showing numbers of genes encoding transcription factors (**E**) and RNA binding proteins (**F**) that were commonly or uniquely down-regulated in the two genotypes.

Down- or up-regulation of *hsrω* transcripts in activated Ras background commonly affected many genes including RNA processing components

The *sev-GAL4>UAS-Ras*^{V12} eye discs showed differential expression of many genes, with 374 being down- and 138 up-regulated, when compared with *sev-GAL4>UAS-GFP* eye discs (List 1 in Fig 5A and B; Supplementary Table S4, Sheet 3). Besides the expected increase in transcripts of cell growth, proliferation and differentiation related genes, many genes involved in RNA biosynthesis, metabolism and processing were also up-regulated when compared with *sev-*

GAL4>UAS-GFP eye discs. Expectedly, *ras* transcripts were significantly higher in *sev-GAL4>UAS-Ras*^{V12}. In agreement with the above RT-PCR results (Supplementary Fig. S1A, B), the RNA seq data also showed that *sev-GAL4* driven down- or up-regulation of *hsrω* lncRNAs in activated Ras expression background did not further increase *ras* transcripts. Further, transcripts of the genes acting directly downstream in Ras signaling cascade were also not up-regulated in eye discs co-expressing *sev-GAL4* driven *UAS-Ras*^{V12} and *hsrωRNAi* or *EP3037* (Supplementary Table S4, sheets 3-5). Eye discs with *sev-GAL4>UAS-Ras*^{V12} expression showed the expected up-regulation of several R7 cell differentiation (*salm, ten-m, cadn, svp, dab, nej*) and photoreceptor development genes (*rno, doa, pdz-gef, jeb, atx2* and *csn4*). However, none of these showed any further change when *hsrωRNAi* or *EP3037* was co-expressed with activated Ras, except for further up-regulation of *svp* in eye discs co-expressing *sev-GAL4* driven activated Ras and *hsrωRNAi* (also see later). The RNA seq data for several of the Ras signaling cascade genes were validated through a real-time qRT-PCR analysis in different genotypes (Supplementary Fig. S1C). In all cases, results of RNA-seq and qRT-PCR were concordant.

We next examined commonly down- or up- regulated genes (Supplementary Table S4, Sheets 4, 5) following expression of *hsrωRNAi* or *EP3037* in *sev-GAL4* driven activated Ras background (encircled in red and white, respectively, in Fig. 5A and B). The group down-regulated by activated Ras expression and further down-regulated by co-expression of *hsrωRNAi* or *EP3037* included only one gene (encircled in red in Fig 5A), while the group up-regulated following activated Ras expression and further up-regulated when *hsrω* RNA levels were altered included three genes (encircled in red in Fig. 5B). The single *CG13900* (*Sf3b3*) gene in the first group encodes a splicing factor, whose role in processing of transcripts, including those in the Ras pathway remains unknown. On basis of their known functions in Flybase, the three up-regulated genes (*CG15630*, *Hsp70Bb* and *CG14516*) in the second group may not be directly involved in modulating Ras pathway.

A group involved in ribosome biogenesis (*CG7275, CG7637, CG14210, hoip, bka, CG11920, CG9344, nhp2, CG11563, mrpl20, CG7006*) was down regulated in activated Ras expressing discs with down-regulated *hsrω* transcripts but was not affected when *EP3037* and activated Ras were co-expressed.

The 88 (9.3%) genes, mostly up-regulated in *sevGAL4>UAS-Ras*^{V12} when compared with *sevGAL4>UAS-GFP* control eye discs, but commonly down-regulated in *sevGAL4>UAS-Ras*^{V12} *hsrωRNAi* or *sevGAL4>Ras*^{V12} *EP3037* compared with *sevGAL4>Ras*^{V12} (encircled in white in Fig. 5A, Fig. 5C-D), encompassed diverse GO terms, mostly without any apparent and known association with Ras signaling. However, the *dlc90F* gene encoding a dynein light chain reportedly binds with Raf (Friedman et al., 2011) and is known to positively regulate FGF signaling (Zhu et al., 2005). Its role in Ras signaling is not known. Several of the 88 genes encoded snoRNA/scaRNA, which were significantly up-regulated by *sevGAL4>UAS-Ras*^{V12} expression but co-expression of either *hsrωRNAi* or *EP3037* led to their significant down-regulation (Fig. 5D). Notablynone of these sno/scaRNAs, except one, were significantly affected

when *hsrωRNAi* or *EP3037* was expressed under the *sev-GAL4* in normal Ras background (Fig. 5D). Interestingly, *sev-GAL4* driven *hsrωRNAi* or *EP3037* expression in normal Ras background affected some other sno/scaRNAs which were not affected by activated Ras expression (data not presented).

The 45 (7%) genes (encircled in white in Fig. 5B, and Fig. 5E) commonly up-regulated following *hsrωRNAi* or *EP3037* co-expression in *sevGAL4>UAS-Ras*^{V12} expressing eye discs compared to those of *sevGAL4>UAS-Ras*^{V12}, were down-regulated or showed no change in *sevGAL4>UAS-Ras*^{V12} when compared with *sevGAL4>UAS-GFP* control discs. This group (Fig. 5B, E) included diverse genes, which may not be directly involved in Ras signaling pathway, except *kuz* (*kuzbanian*), encoding a metalloprotease expressed in developing ommatidia with roles in neuroblast fate determination, round-about (Robo) signaling and neuron formation (Coleman et al., 2010; Sotillos et al., 1997; Udolph et al., 2009). Therefore, its up-regulation in discs with altered *hsrω* RNA levels in activated Ras background may contribute to more R7 photoreceptor/neuronal cells.

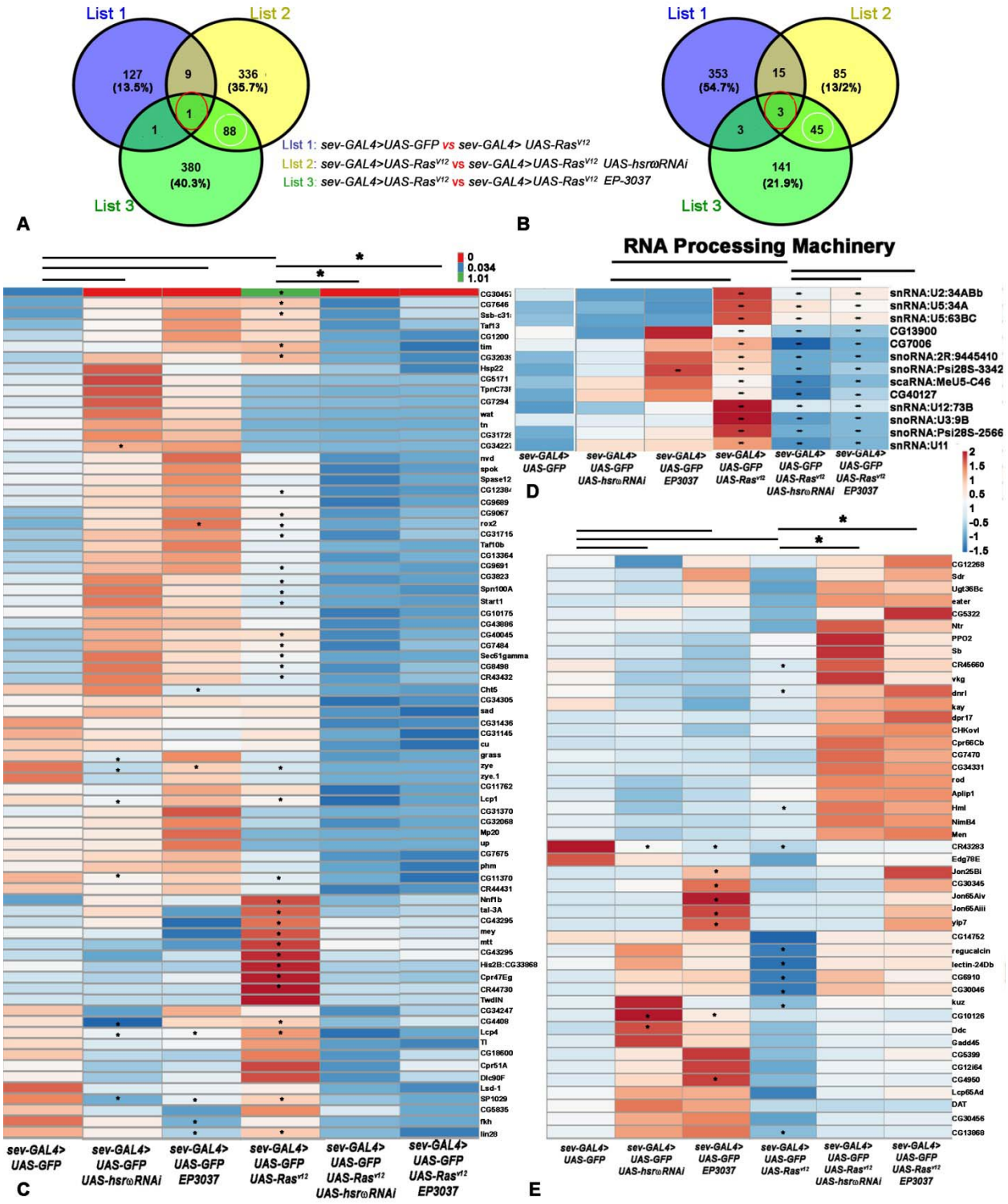

Fig. 5. Many transcripts, which were significantly up- or down-regulated following *sev-GAL4>*activated Ras expression, showed commonly opposite changes following either reduction or elevation of *hsrω* RNAs. A-B Venn diagrams showing numbers of genes down- (**A**) or up- (**B**) regulated in eye discs with either decreased (List 2) or increased (List 3) levels of

hsrω RNA in activated Ras expression background as compared to control (*sev-GAL4>UAS-Ras*^{V12} vs *sev-GAL4>UAS-GFP*, List 1). **C-D** Heat maps of FPKM values of different transcripts (noted on right of each row) of diverse GO terms (**C**) or RNA processing machinery (**D**) in different genotypes (noted at base of each column) which, compared to *sev-GAL4>UAS-GFP* (column 1), were unaffected or up-regulated in *sev-GAL4>*activated Ras expressing discs (column 4) but were significantly down-regulated following co-expression of *sev-GAL4>*activated Ras and altered *hsrω* RNA levels (columns 5 and 6). **E** Heat maps of FPKM values of genes which were unaffected or down-regulated following activated Ras expression but significantly up-regulated in eye discs co-expressing activated Ras and co-altered *hsrω* RNA levels. Heat maps of transcripts in *sev-GAL4>UAS-GFP* (column 1), *sev-GAL4>UAS-hsrωRNAi* (column 2) and *sev-GAL4>EP-3037* (column 3) are also shown for comparison. Asterisks indicate significant differences ($p \leq 0.05$) between the compared genotypes connected by horizontal lines on top; the Asterisk marks above horizontal lines connecting columns 4-5 and 4-6 in **C-E** indicate significant differences in all genes in the columns. Colour key for expression levels for the top row in **C** is above **C,** while that for all others is on middle right.

Finally, we examined genes that were differentially affected when *hsrωRNAi* or *EP3037* were co-expressed with activated Ras. These belonged to different pathways, but one significant group included positive and negative modulators of Ras signaling and photoreceptor differentiation (Fig. 6). The GO search revealed enhanced levels of positive modulators Ras signaling in R7 cell fate determination (*phly, svp, rau* and *socs36E*) in *sevGAL4>UAS-Ras*^{V12} *UAS-hsrωi* discs compared to *sevGAL4>UAS-Ras*^{V12} discs (Fig. 6). None of these four genes were up-regulated in *sevGAL4>UAS-Ras*^{V12} *EP3037* background (Fig. 6). However, several negative regulators of Ras signal transduction pathway (*bru, klu, mesr4, cdep, epac,, nfat, ptp-er, cg43102, rhogap1a, rhogef2, spri, exn* etc were down regulated (Fig 6) in *sev-GAL4>UAS-Ras*^{V12} *EP3037* but not in *sev-GAL4>UAS-Ras*^{V12}*UAS-hsrωRNAi* eye discs. On the basis of David Bioinformatics GO terms, genes like *bru, cdep, sos, pdz-gef, cg43102, rhogap1a, rhogef2, spri, exn* are involved in Ras guanyl nucleotide exchange factor activity while genes like *klu, mesr4, nfat, ptp-er* affect small GTPase mediated signal transduction. Being negative-regulators, their down-regulation by co-expression of activated Ras and *EP3037* would further enhance Ras activity. Interestingly, in normal developmental Ras activity background, the *sev-GAL4>UAS-hsrωRNAi* or *EP3037* expression did not differentially affect expression of these positive and negative Ras signaling modulators since columns 2 and 3 in Fig. 6 show that most of them were either not affected or were commonly down regulated when compared with *sev-GAL4>UAS-GFP* eye discs.

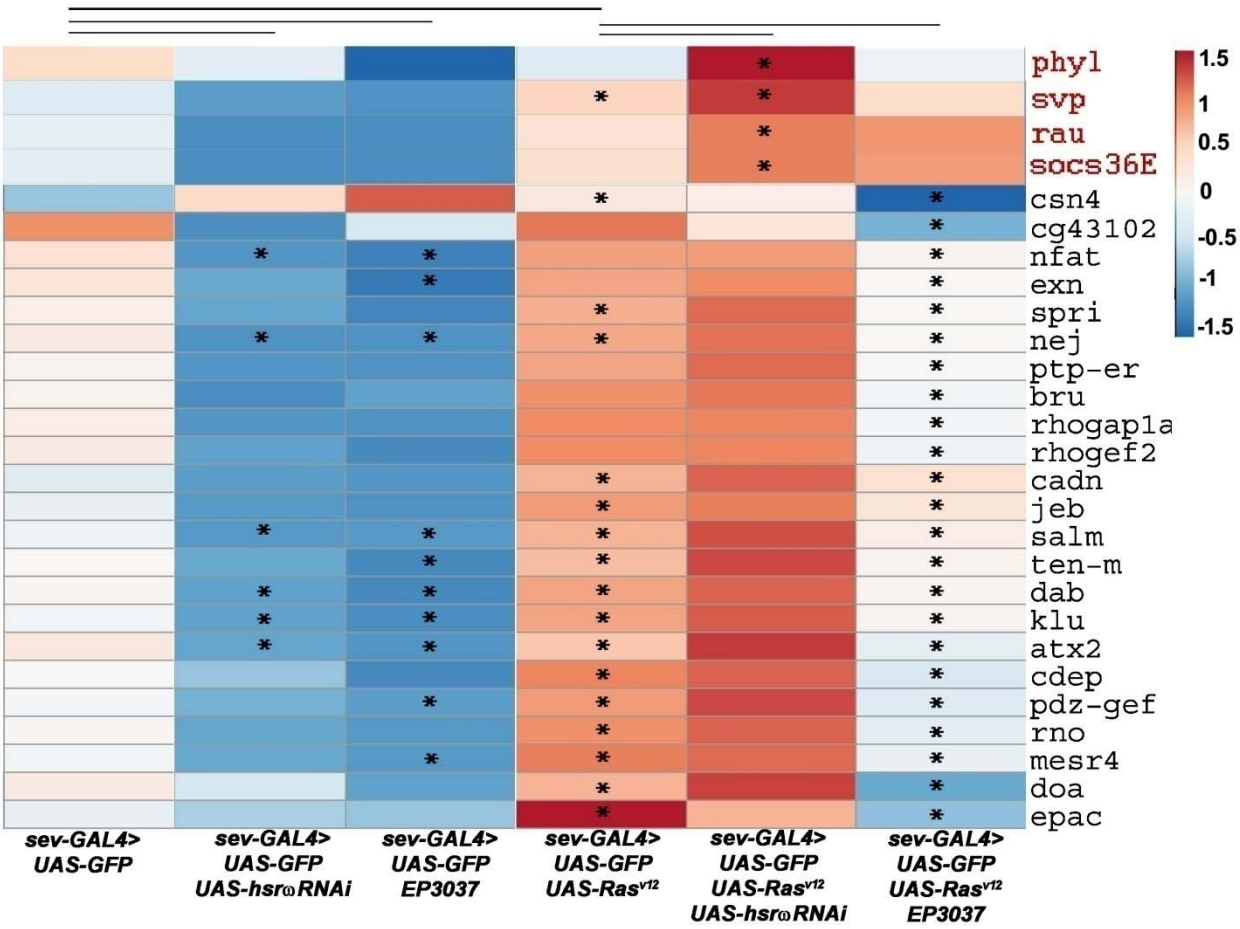

Fig. 6. Transcripts of positive Ras modulators are up-regulated while negative modulators are down-regulated upon down- and up-regulation, respectively, of *hsrω* transcripts in activated Ras expression background. Heat maps of FPKM values of Ras signaling and photoreceptor differentiation transcripts (noted on right of each row) in different genotypes. The four potential positive modulators of Ras signaling are in red fonts. Asterisks indicate significant differences ($p \leq 0.05$) between the compared genotypes connected by horizontal lines on top.

Many transcription factor and RNA-binding protein genes were affected by altered *hsrω* transcript levels in activated Ras background

We examined activities of genes encoding TF and RBP in different genotypes to examine if the elevated Ras signaling in eye discs co-expressing *sev-GAL4* driven activated Ras and altered *hsrω* transcripts levels could be due to altered activities of genes affecting transcription and post-transcriptional processing of gene transcripts encoding proteins that modulate Ras signaling.

Out of ~1000 known TF (Rhee et al., 2014) in *Drosophila melanogaster*, 29 and 81 showed differential expression in *sev-GAL4>UAS-Ras^{V12} UAS-hsrωRNAi* and *sev-GAL4>UAS-Ras^{V12} EP3037*, respectively, when compared with *sev-GAL4>UAS-Ras^{V12}* (Fig. 7A, B). While 73 TF genes were uniquely down regulated in *sev-GAL4>UAS-Ras^{V12} EP3037*, only 9 were down-

regulated in *sev-GAL4>UAS-Ras^{V12} UAS-hsrωRNAi* (Fig. 7A). On the other hand, compared to 14 TF genes uniquely up-regulated in *sev-GAL4>UAS-Ras^{V12} UAS-hsrωRNAi*, *EP3037* expression in *GAL4>UAS-Ras^{V12}* background enhanced only 2 (Fig. 7B). Fewer TF were commonly down- or up- regulated, being 4 (*CG11762/ouijaboard*, *lin-28*, *forkhead*, *Ssb-c31a*) and 2 (*Ets21C* and *kay*), respectively (Fig. 7A, B). *CG11762* and *forkhead* are part of the ecdysone signaling pathway (Cao et al., 2007; Komura-Kawa et al., 2015). Ssb-c31a, as noted earlier, reportedly binds with Raf. The two commonly up-regulated TF are part of JNK pathway. GO search showed, as noted earlier (Fig. 6), that three TF, viz., Klu, Mesr4, Nfat, uniquely down-regulated in *sev-GAL4>UAS-Ras^{V12} UAS*-EP3037 (Fig. 7F), are negative regulators of Ras signaling. On the other hand, five TF, viz., Svp, Peb, Gl, Ro and H, up-regulated in *sev-GAL4>UAS-Ras^{V12} UAS-hsrωRNAi* (Fig. 7 E), are involved in rhabdomere differentiation (Frankfort and Mardon, 2002; Kimmel et al., 1990; Kumar and Moses, 2000; Liang et al., 2016; Moses et al., 1989; Pickup et al., 2002).

Comparison of levels of known RBP (RNA binding protein Database at http://rbpdb.ccbr.utoronto.ca) in eye discs expressing activated Ras alone or along with changes in *hsrω* RNA levels showed that 9 and 13 RBP genes were uniquely down-regulated when *hsrω* RNAs were down-or up-regulated, respectively, in activated Ras background. Two genes, *CG7006* (a ribosome biogenesis factor NIP7-like) and *lin-28*, regulating maturation of let-7 microRNA (Moss and Tang, 2003; Newman et al., 2008; Stratoulias et al., 2014; Viswanathan et al., 2008), were commonly down-regulated following alteration of *hsrω* transcripts in *sevGAL4>UAS-Ras^{V12}* (Fig 7C). Only *cpo* was uniquely up-regulated in *sev-GAL4>UAS-Ras^{V12} UAS-hsrωRNAi*. Likewise, only *fne* was up-regulated in *sev-GAL4>UAS-Ras^{V12} EP-3037* eye discs. Interestingly, transcripts of most of the known omega speckle associated RBP showed no change in any of the three activated Ras genotypes examined here (Fig. 7D).

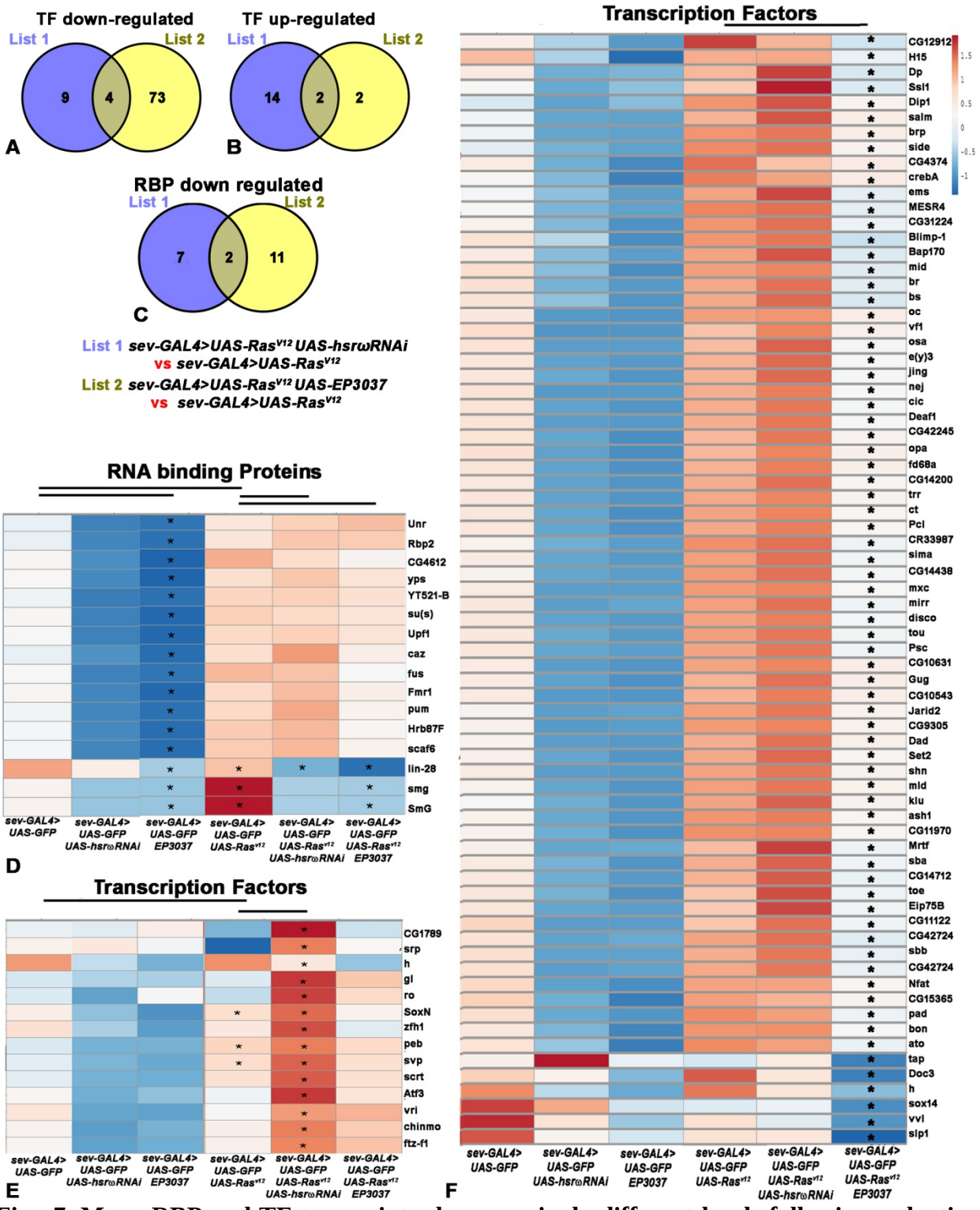

Fig. 7. Many RBP and TF transcripts show varyingly different levels following reduction or enhancement of *hsrω* transcripts in activated Ras than in normal Ras background. A-B Venn diagrams showing numbers of TF genes down- (**A**) or up-regulated (**B**) following either decrease (List1) or increase (List2) in *hsrω* RNA levels in *sev-GAL4>UAS-Ras*^{V12} background compared to *sev-GAL4>UAS-Ras*^{V12}. **C** Venn diagrams showing numbers of RBP genes down-

regulated following either decrease (List1) or increase (List 2) in *hsrω* RNA levels in *sev-GAL4>UAS-Ras^{V12}* compared with *sevGAL4>UAS-Ras^{V12}* discs. **D** Heat maps of FPKM values of different RBP transcripts (noted on right of each row) in different genotypes (noted below each column) which were significantly down-regulated in *sev-GAL4>EP3037* compared to *sev-GAL4>UAS-GFP*. **E-F** Heat maps of FPKM values of TF transcripts in different genotypes (below each column) which were either significantly up-regulated in activated Ras and lowered *hsrω* RNA levels when compared to only activated Ras expressing eye discs (**E**) or significantly down-regulated in activated Ras and enhanced *hsrω* RNA levels (**F**). Asterisks indicate significant differences ($p \leq 0.05$) between the compared genotypes (indicated by the horizontal lines at the top.

Discussion

Present study was initiated to examine interactions between *hsrω* lncRNAs and Ras signaling cascade. Although oncogenic Ras is reported to influence expression of several lncRNAs (Jiang et al., 2017; Jinesh et al., 2018; Kotake et al., 2016; Rotblat et al., 2011; Zhang et al., 2017b), regulation of Ras signaling by lncRNAs is not known. Following an earlier study from our lab that a *ras* mutant allele enhanced *hsrω*-null phenotype (Ray and Lakhotia, 1998), present study shows that alterations in levels of *hsrω* transcripts exaggerate phenotypes that follow the *sev-GAL4* driven expression of activated Ras in developing eye discs of *Drosophila*. The *UAS-Ras^{V12}* transgene (Karim et al., 1996) is widely used for examining consequence of ectopic expression of ligand-independent activated Ras. Its expression in eye discs under the *sev-GAL4* driver disrupts ommatidial arrays by recruitment of additional cells to R7 photoreceptor path (Karim et al., 1996). Our results clearly show that reduced as well as over-expressed *hsrω* transcripts in activated Ras background significantly enhanced R7 photoreceptor number per ommatidium. As revealed by detection of pMAPK, Yan and activated Ras associated RafRBDFLAG in eye discs, the increase in R7 photoreceptors distinctly correlated with the enhanced Ras activity levels in *sev-GAL4> UAS-Ras^{V12} hsrωRNAi* and *sev-GAL4> UAS-Ras^{V12} EP3037* genotypes.

The similar enhancing effect of down- or up-regulation of *hsrω* transcripts on Ras signaling appears incongruous. In order to rule out non-specific effects, we down-regulated *hsrω* through a different *UAS-pUHEx2A* RNAi transgene (R. R. Sahu and S. C. Lakhotia, unpublished) that targets a region (exon 2) common to all *hsrω* transcripts (Lakhotia, 2017a), and a different allele, *EP93D* (Mallik and Lakhotia, 2009), to over-express *hsrω*. In each case, the Ras signaling was comparably enhanced when these were co-expressed with *sev-GAL4>UAS-Ras^{V12}*. We also found increased R7 photoreceptors and greater roughening of eyes following *sev-GAL4>UAS-Ras^{V12}* expression in *hsrω^{66}* (a near-null allele of *hsrω*) background (data not presented) confirming enhanced Ras activity following reduction of *hsrω* transcripts. These *hsrωRNAi* and *EP* lines have been used in several studies (Lakhotia et al., 2012; Mallik and Lakhotia, 2009; Mallik and Lakhotia, 2010; Mallik and Lakhotia, 2011; Onorati et al., 2011; Piccolo et al., 2018; Piccolo and Yamaguchi, 2017; Singh and Lakhotia, 2015) without any nonspecific effects, although similar as well as dissimilar end-phenotypes were seen under different conditions

following down- or up-regulation of the *hsrω* gene expression. Together, these confirm that the similar end-result of down- or up-regulation of *hsrω* transcripts on Ras signaling in high activated Ras background reflects specific consequences of the complex interactions between ectopically expressed activated Ras and altered levels of *hsrω* lncRNAs.

Down- or up-regulation of *hsrω* transcripts in wild type Ras background does not affect ommatidial differentiation since *sev-GAL4>UAS-hsrωRNAi* or *sev-GAL4>EP3037* flies show normal eyes without extra rhabdomeres (Mallik and Lakhotia, 2011). Moreover, Ras and RafRBDFLAG immunostaining in *sev-GAL4>UAS-GFP* or *sevGAL4>UAS-hsrωRNAi* or *sev-GAL4>EP3037* eye discs also did not show any difference between them (not shown). Apparently, ectopic over-expression of activated Ras makes ommaidial differentiation detectably sensitive to altered *hsrω* transcript levels.

Since the *sev-GAL4>UAS-Ras^{V12} UAS-hsrωRNAi* or *sev-GAL4>UAS-Ras^{V12} EP3037* eye discs did not show altered *Ras* or *Ras^{V12}* transcript levels despite significantly enhanced total as well as activated Ras protein levels (Fig. 3), we believe that altered *hsrω* transcript levels further enhance Ras activity when activated Ras is already high through modulation of activities of other regulators of the Ras cascade. Our data show (Fig. 6) significantly elevated transcripts of some positive modulators of Ras activity in R7 differentiation (*phly, svp, rau* and *socs36E*) in *sev-GAL4>Ras^{V12} UAS-hsrωRNAi* eye discs. The *phly* encodes a nuclear receptor acting downstream of Ras in R7 fate determination (Chang et al., 1995). Svp is an orphan nuclear receptor responsible for transforming cone cells to R7 photoreceptor in conjunction with activated Ras (Begemann et al., 1995; Kramer et al., 1995). Svp expression also increases Rau expression, which sustains RTK signaling (Sieglitz et al., 2013). The Socs36E amplifies Ras/MAPK signaling in R7 precursors (Almudi et al., 2010). Genes like *bru, cdep, sos, pdz-gef, cg43102, rhogap1a, rhogef2, spri, exn*, which appeared down regulated in *sev-GAL4>UAS-Ras^{V12}UAS-EP3037* eye discs, are involved in Ras guanyl nucleotide exchange factor activity (Jékely et al., 2005; Lee et al., 2002; Yan and Perrimon, 2015) while *klu, mesr4, nfat, ptp-er* are negative regulators of small GTPase mediated signal transduction (Ashton-Beaucage et al., 2014; Brachmann and Cagan, 2003; Huang and Rubin, 2000). Thus the net result in *sev-GAL4>UAS-Ras^{V12} UAS-hsrωRNAi* as well as *sev-GAL4>UAS-Ras^{V12} UAS-EP3037* discs would be up-regulation of Ras activity. The positive regulators may have stronger action than the negative modulators and thus may contribute to the greater enhancement in Ras signaling in *sev-GAL4>Ras^{V12} UAS-hsrωRNAi* eye discs. The observed up-regulation of Ssb-c31a in *sev-GAL4>Ras^{V12}UAS-hsrωRNAi* and *sev-GAL4>Ras^{V12}UAS-EP3037* can also contribute to the elevated Ras signaling through its binding with Raf (Friedman et al., 2011).

Since the *hsrω* transcripts do not bind with gene promoters or other RNAs, the changes in activities of the negative and positive modulators of Ras signaling appear to be mediated through activities of the diverse proteins that associate with *hsrω* lncRNAs. Of the multiple *hsrω* transcripts (Lakhotia, 2011; Lakhotia, 2017b), the >10kb nucleus-limited transcripts are essential for biogenesis of omega speckles and consequently for the dynamic movement of omega speckle

associated proteins like various hnRNPs, some other RBP and nuclear matrix proteins etc (Lakhotia et al., 2012; Mallik and Lakhotia, 2011; Piccolo et al., 2018; Piccolo and Yamaguchi, 2017; Singh and Lakhotia, 2015). The GAL4 induced expression of *hsrωRNAi* transgene or the *EP3037 hsrω* allele primarily lowers and elevates, respectively, levels of nucleus-limited larger *hsrω* transcripts (Mallik and Lakhotia, 2009)(Mallik and Lakhotia, 2011). Either of these disrupt omega speckles and dynamics of their associated RBP (Lakhotia et al., 2012; Piccolo et al., 2018; Piccolo and Yamaguchi, 2017; Singh and Lakhotia, 2015). Because of multiple and diverse roles of these proteins in gene expression and post-transcriptional processing/stability of diverse RNAs, the *hsrω* lncRNAs behave like hubs in complex cellular networks (Arya et al., 2007; Lakhotia, 2012; Lakhotia, 2016). Commonly disrupted dynamics of several important RBP following down- or up-regulation of *hsrω* transcripts may indeed underlie the unexpected commonality in enhancing Ras signaling cascade by down- and up-regulation of *hsrω* transcript levels in high activated Ras expression background. Our transcriptomic data agrees with this.

The Caz/dFus hnRNP family member protein interacts with omega speckles and moves out to cytoplasm following down regulation of *hsrω* transcripts (Piccolo and Yamaguchi, 2017). We found *EP3037* expression reduced *Caz/dFus* transcripts. A bioinformatic search (data not presented) revealed that transcripts of many of the positive and negative modulators of Ras signaling, whose levels were enhanced or reduced (Fig.6) in discs with altered *hsrω* activity and high activated Ras, indeed carry binding sites for Caz/dFus. Significantly, TDP-43 (dTBPH), another hnRNP, interacts with omega speckles and with Caz/dFus (Appocher et al., 2017; Coyne et al., 2015; Piccolo et al., 2018; Romano et al., 2014). Both of these interact with Fmr1 RBP. Their complex interactions variably affect processing, translatability and stability of diverse mRNAs (Appocher et al., 2017; Coyne et al., 2015; Piccolo et al., 2018; Piccolo and Yamaguchi, 2017; Romano et al., 2014). Many genes of the Ras pathway were also differentially expressed in Caz/dFus depleted mouse cell lines (Honda et al., 2014). Like many other RBP, these three genes produce multiple transcripts and multiple protein products (http://Flybase.org). Thus depending upon the context, the *hsrω* interacting proteins can affect different sets of transcripts differently by modulating their abundance, translatability and turnover etc. Notably, like the similar end-results of down- and up-regulation of *hsrω* transcripts noted in our study, wild type dFus over-expression as well as mutant dFus expression are associated with Frontotemporal Dementia and Amyotrophic Lateral Sclerosis (Machamer et al., 2018).

The *let-7* miRNA binds with 3'UTR of *ras* transcripts and is lowered by high Ras levels and vice-versa (Jinesh et al., 2018; Johnson et al., 2005; Wang et al., 2013). Interestingly, *let-7* pre- and mature miRNA also bind with *TDP-43* and *Fmr1* transcripts and TDP-43 knock down reduces *let-7b* miRNA (Buratti et al., 2010; Yang et al., 2009)(Buratti et al., 2010; Chen et al., 2017; Kumar et al., 2016). TDP-43's movement away from nucleus to cytoplasm in *hsrω* RNA depleted condition (Piccolo et al., 2018) may reduce functional *let-7* availability and consequently enhance Ras activity. Since Lin-28 regulates *let-7* maturation (Moss and Tang, 2003; Newman et al., 2008; Stratoulias et al., 2014; Viswanathan et al., 2008), the observed up-

regulation of *Lin-28* transcripts in *sev-GAL4>UAS-Ras^{V12} UAS-hsrωRNAi* and *sev-GAL4>UAS-Ras^{V12} UAS-EP3037* eye discs too can affect *let-7* miRNA activity and consequently, Ras levels.

The *hsrω* RNA levels directly or indirectly also affect small ncRNAs since snoRNAs, snRNAs and scaRNAs, which were highly up regulated in activated Ras background, were significantly down-regulated following co-alteration of *hsrω* transcript levels. Besides their roles in maturation of rRNAs (Dieci et al., 2009; Dragon et al., 2006; Henras et al., 2015; Sloan et al., 2017), snoRNAs also modify some snRNAs (Dupuis-Sandoval et al., 2015; Falaleeva and Stamm, 2013; McMahon et al., 2015). The Cajal body associated scaRNAs are essential for functioning and maturation of snRNAs and thus critical for mRNA processing (Darzacq et al., 2002; Deryusheva and Gall, 2009; Kiss et al., 2002; Kiss, 2004; Richard et al., 2003). Therefore, sca, sn and snoRNAs can profoundly affect transcriptional and translational activities. Loss of two snoRNAs, SNORD50A and SNORD50B, in human cells is associated with increased hyperactivated Ras/ERK signaling (Siprashvili et al., 2016). The possibility of involvement of such small ncRNAs enhancing Ras signaling, especially in altered *hsrω* transcript levels, needs further examination. Significance of the observed greater reduction in some ribosomal protein transcripts in *sev-GAL4>Ras^{V12} UAS-hsrωRNAi* eye discs also needs further studies in the context of reported reduction of some ribosomal proteins following activation of Ras pathway (Friedman et al., 2011). Likewise, roles, if any, of altered expression of *CG13900*, *dlc90F* and *kuz* in further elevating the Ras signaling in the experimental genotypes remains to be examined.

Several studies (Enomoto et al., 2015; Parry and Sundaram, 2014; Takino et al., 2014; Uhlirova et al., 2005; Yan et al., 2009) have provided evidence for cell non-autonomous Ras signaling, including transfer of GFP tagged H-Ras from antigen-presenting cells to T cells (Goldstein et al., 2014). The observed presence of *sev-GAL4* driven RafRBDFLAG bound Ras in neighboring non *sev-GAL4* expressing cells suggests similar movement of activated Ras-Raf complex from source cells to neighbors. The cell non-autonomous Ras signaling is also indicated by the greatly reduced Yan expression even in MF region.

Our findings, besides highlighting roles of non-coding part of the genome in modulating important signaling pathway like Ras, also unravel new insights into working of Ras signaling cascade itself. The observed non cell-autonomous spread of Ras signaling and further enhancement in the already elevated Ras activity by lncRNA assume significance in view of roles of activated Ras/Raf mutations in diverse malignancies. Future studies on interactions between the diverse small and long ncRNAs and signaling pathways like Ras would unravel new dimensions of cellular networks that regulate and determine basic biological processes on one hand, and cancer on the other.

Materials and Methods

Fly stocks

All fly stocks and crosses were maintained on standard agar-maize powder-yeast and sugar food at 24±1^{0}C. The following stocks were obtained from the Bloomington Stock Centre (USA): *w^{1118}; sev-GAL4; +* (no. 5793; Bailey 1999), *w^{1118}; UAS-GFP* (no. 1521), *w^{1118}; UAS-Ras^{V12}* (no. 4847). For targeted (Brand and Perrimon, 1993) down-regulation of the hsrω transcripts, *UAS-hsrω-RNAi^3* transgenic line (Mallik and Lakhotia, 2009) was used; in some cases another RNAi transgene, *UAS-pUHEx2ARNAi*, which targets the exon 2 region of the *hsrω* gene (R. R. Sahu and S. C. Lakhotia, unpublished) was also used. Up regulation of the *hsrω* was achieved by expressing *EP3037* allele, or in a few cases the *EP93D* allele, under the *sev-GAL4* driver (Mallik and Lakhotia, 2009). The *UAS-hsrω-RNAi^3* and the *EP3037* lines are referred to in the text as *UAS-hsrωRNAi* and *EP3037*, respectively. The *UAS-RafRBDFLAG* stock (Freeman et al., 2010) was provided by Dr. S. Sanyal (Emory University, USA). Using these stocks, appropriate crosses were made to finally obtain progenies of the following genotypes:

a) *w^{1118};* sev-GAL4 *UAS-GFP/UAS-GFP; dco^2 e/+*

b*) w^{1118}; sev-GAL4 UAS-GFP/UAS-GFP; dco^2 e/UAS- Ras^{V12}*

c*) w^{1118}; sev-GAL4 UAS-GFP/UAS-GFP; UAS-hsrωRNAi/UAS-Ras^{V12}*

d) *w^{1118}; sev-GAL4 UAS-GFP/UAS-GFP; EP3037/UAS-Ras^{V12}*

e*) w^{1118}; sev-GAL4 UAS-GFP/UAS-GFP; EP93D/UAS-Ras^{V12}*

f*) w^{1118}; sev-GAL4 UAS-GFP/UAS-pUHEx2ARNAi; +/UAS-Ras^{V12}*

h) *w^{1118};* sev-GAL4 *UAS-GFP/UAS-RafRBDFLAG; dco^2 e/+*

i) *w^{1118}; sev-GAL4 UAS-GFP/UAS-RafRBDFLAG; dco^2 e/UAS-Ras^{V12}*

j) *w^{1118}; sev-GAL4 UAS-GFP/UAS-RafRBDFLAG; UAS-hsrωRNAi/UAS-Ras^{V12}*

k) *w^{1118}; sev-GAL4 UAS-GFP/UAS-RafRBDFLAG; EP3037/UAS-Ras^{V12}*

The *w^{1118}*, *dco^2* and *e* markers are not mentioned while writing genotypes in Results.

Lethality Assay

For lethality assay, freshly hatched 1st instar larvae of *sev-GAL4>UAS-GFP*, *sev-GAL4>Ras^{V12}*, *sev-GAL4>UAS-Ras^{V12}UAS-hsrωRNAi* and *sev-GAL4>UAS-Ras^{V12}EP3037* were collected during one hour interval and gently transferred to food vials containing regular food and reared at 24±1°C or at 18±1°C. The total numbers of larvae that pupated and subsequently emerged as flies were counted for at least three replicates of each experimental condition and/or genotypes.

Photomicrography of adult eyes

For examining the external morphology of adult eyes, flies of the desired genotypes were etherized and their eyes photographed using a Sony Digital Camera (DSC-75) attached to a Zeiss Stemi SV6 stereobinocular microscope or using Nikon Digital Sight DS-Fi2 camera mounted on Nikon SMZ800N stereobinocular microscope.

Nail polish imprints

The flies to be examined for organization of ommatidial arrays were anaesthetized and decapitated with needle and the decapitated head was briefly dipped in a drop of transparent nail polish placed on a slide. It was allowed to dry at RT for 5-10 min after which the dried layer of nail polish was carefully separated from the eye tissue with the help of fine dissecting needles and carefully placed on another clean glass slide with the imprint side facing up and flattened by gently placing a cover slip over it as described earlier (Arya and Lakhotia, 2006). The eye imprints were examined using 20X DIC optics.

Whole organ immunostaining

Eye discs from actively migrating late third instar larvae of desired genotypes were dissected out in PSS and immediately fixed in freshly prepared 3.7%paraformaldehyde in PBS for 20 min and processed for immunostaining as described earlier (Prasanth et al., 2000). The following primary antibodies were used: rat monoclonal anti-Elav (DSHB, 7E8A10, 1:100), rabbit monoclonal anti-Ras (27H5, Cell signaling, 1:50), mouse anti-FLAG M2 (Sigma-Aldrich, India, 1:50), rabbit p-MAPK (Phospho-p44/42 MAPK (Thr202, Tyr204), D13.14.4E, Cell signaling, 1:200), mouse anti-Yan (8B12H9, Developmental Studies Hybridoma Bank, Iowa, 1:100) and guinea pig anti-Runt, a gift by Dr. K. Vijaya Raghavan, India, (Kosman et al., 1998) at 1:200 dilution. Appropriate secondary antibodies conjugated either with Cy3 (1:200, Sigma-Aldrich, India) or Alexa Fluor 633 (1:200; Molecular Probes, USA) or Alexa Fluor 546 (1:200; Molecular Probes, USA) were used to detect the given primary antibodies. Chromatin was counterstained with DAPI (4', 6-diamidino-2-phenylindole dihydrochloride, 1µg/ml). Tissues were mounted in DABCO antifade mountant for confocal microscopy with Zeiss LSM Meta 510 using Plan-Apo 40X (1.3-NA) or 63X (1.4-NA) oil immersion objectives. Quantitative estimates of proteins in different regions of eye discs and co-localization were obtained, when required, with the help of Histo option of the Zeiss LSM Meta 510 software. All images were assembled using the Adobe Photoshop 7.0 software.

RNA isolation and Reverse Transcription-PCR

For semi-quantitative RT-PCR and qRT-PCR analyses, total RNA was isolated from eye imaginal discs of healthy wandering third instar larvae of the desired genotypes using Trizol reagent following the manufacturer's (Sigma-Aldrich, India) recommended protocol. RNA pellets were resuspended in nuclease-free water and quantity of RNA was estimated

spectrophotometrically. The RNA samples (1µg) were incubated with 2U of RNase free DNaseI (MBI Fermentas, USA) for 30 min at 37°C to remove any residual DNA. First strand cDNA was synthesized from 1-2 µg of total RNA as described earlier (Mallik and Lakhotia, 2009). The prepared cDNAs were subjected to semi quantitative RT-PCR or real time PCR using forward and reverse primer pairs (see Supplementary Table S3). Real time qPCR was performed using 5µl qPCR Master Mix (SYBR Green, Thermo Scientific), 2 picomol/µl of each primer per reaction in 10 µl of final volume in an ABI 7500 Real time PCR machine.

The PCR amplification reactions were carried out in a final volume of 25 µl containing cDNA (50 ng), 25 pM each of the two specified primers, 200 µM of each dNTPs (Sigma Aldrich, USA) and 1.5U of *Taq* DNA Polymerase (Geneaid, Bangalore). The cycling parameters for specific transcripts are given in Supplementary Table S3**.** 15 µl of the PCR products were loaded on a 2% agarose gel to check for amplification along with a 50bp DNA ladder as a molecular marker.

Next Generation RNA sequencing

Total RNA was isolated from 30 pairs of eye discs of *sev-GAL4>UAS-GFP*, *sev-GAL4>UAS-hsrωRNAi*, *sev-GAL4>EP3037*, *sev-GAL4>UAS-Ras^{V12}*, *sev-GAL4>UAS-hsrωRNAi UAS-Ras^{V12}* and *sev-GAL4>EP3037 UAS-Ras^{V12}* late third instar larvae using Trizol (Invitrogen, USA) reagent as per manufacture's protocol. 1µg of the isolated RNA was subjected to DNAse treatment using 2U of TurboTM DNAse (Ambion, Applied Biosystem) enzyme for 30 min at 37°C. The reaction was stopped using 15mM EDTA followed by incubation at 65°C for 5-7 min and purification on RNAeasy column (Qiagen). The purified RNA samples were processed for preparations of cDNA libraries using the TruSeq Stranded Total RNA Ribo-Zero H/M/R (Illumina) and sequenced on HiSeq-2500 platform (Illumina) using 50bp pair-end reads, 12 samples per lane and each sample run across 2 lanes. This resulted in a sequencing depth of ~20 million reads. Biological triplicate samples were sequenced in each case. The resulting sequencing FastQ files were mapped to the *Drosophila* genome (dm6) using Tophat with Bowtie. The aligned SAM/BAM file for each was processed for guided transcript assembly using Cufflink 2.1.1 and gene counts were determined. Mapped reads were assembled using Cufflinks. Transcripts from all samples were subjected to Cuffmerge to get final transcriptome assembly across samples. In order to ascertain differential expression of gene transcripts between different samples, Cuffdiff 2.1.1 was used (Trapnell et al., 2012). A P-value <0.05 was taken to indicate significantly differentially expressing genes between different groups compared. Genes differentially expressed between experimental and control genotypes were categorized into various GO terms using DAVID bioinformatics Resources 6.8 (Huang et al., 2009) https://david.ncifcrf.gov for gene ontology search. In order to find out distribution of differentially expressing genes into various groups, Venn diagrams and Heat maps were prepared using the Venny2.1 and ClustVis softwares, respectively (Metsalu and Vilo, 2015).

The RNA sequence data files, showing pair wise comparisons of gene expression levels for different genotypes are presented in Supplementary Table S3

Acknowledgements

We thank the Bloomington *Drosophila* Stock Ctr and Drs S. Sanyal (Emory University, USA) and Dr. Stephen W. Mckechnie (Australia) for providing fly stocks. We thank Developmental Studies Hybridoma Bank (DSHB, Iowa, USA) for anti-Elav and anti-Yan, and Dr. K. Vijay Raghavan (India) for anti-Runt antibodies. We thank the Department of Biotechnology, Govt. of India (New Delhi) and the Indian Council of Medical Research (New Delhi) for supporting this research. We also thank the Centre of Advanced Studies in Department of Zoology, DBT-BHU Interdisciplinary School of Life Sciences and the Centre of Genetic Disorders (CGD) at BHU for various facilities. Special thanks to Dr Amit Chaurasia of Premas Biotech, CGD, for RNA-sequencing. We acknowledge the Department of Science & Technology, Govt. of India (New Delhi) and the Banaras Hindu University for Confocal Microscopy facility.

Competing interests

Authors declare no conflicting interests

Author contributions

MR and SCL planned experiments, analyzed results and wrote the manuscript. MR carried out the experimental work and collected data.

Funding

This work was supported by a CEIB-II grant from the Department of Biotechnology, Govt. of India to SCL. MR was supported as senior research fellow by the Indian Council of Medical Research, New Delhi, India.

Data availability

The NGS data for RNA-sequencing in activated Ras expressing genotypes have been deposited at GEO (http://www.ncbi.nlm.nih.gov/geo/) with accession no. GSE107529. RNA-seq data for eye discs with *sev-GAL4* driven altered levels of *hsrω* transcripts in normal Ras background have been deposited at GEO (http://www.ncbi.nlm.nih.gov/geo/) with accession no. GSE116476.

References

Almudi, I., Corominas, M. and Serras, F. (2010). Competition between SOCS36E and Drk modulates Sevenless receptor tyrosine kinase activity. *J Cell Sci* **123**, 3857-3862.

Appocher, C., Mohagheghi, F., Cappelli, S., Stuani, C., Romano, M., Feiguin, F. and Buratti, E. (2017). Major hnRNP proteins act as general TDP-43 functional modifiers both in Drosophila and human neuronal cells. *Nucleic Acids Research* **45**, 8026-8045.

Arya, R. and Lakhotia, S. (2006). A simple nail polish imprint technique for examination of external morphology of Drosophila eyes. *Current science* **90**, 1179-1180.

Arya, R., Mallik, M. and Lakhotia, S. (2007). Heat shock genes - integrating cell survival and death. *Journal of Biosciences* **32**, 595-610.

Ashton-Beaucage, D., Udell, C. M., Gendron, P., Sahmi, M., Lefrançois, M., Baril, C., Guenier, A.-S., Duchaine, J., Lamarre, D. and Lemieux, S. (2014). A functional screen reveals an extensive layer of transcriptional and splicing control underlying RAS/MAPK signaling in Drosophila. *PLoS biology* **12**, e1001809.

Begemann, G., Michon, A.-M., vd Voorn, L., Wepf, R. and Mlodzik, M. (1995). The Drosophila orphan nuclear receptor seven-up requires the Ras pathway for its function in photoreceptor determination. *Development* **121**, 225-235.

Brachmann, C. B. and Cagan, R. L. (2003). Patterning the fly eye: the role of apoptosis. *TRENDS in Genetics* **19**, 91-96.

Brand, A. H., Manoukian, A. S. and Perrimon, N. (1994). Ectopic expression in Drosophila. *Methods in cell biology* **44**, 635-654.

Brand, A. H. and Perrimon, N. (1993). Targeted gene expression as a means of altering cell fates and generating dominant phenotypes. *development* **118**, 401-415.

Brunner, D., Dücker, K., Oellers, N., Hafen, E., Scholzi, H. and Klambt, C. (1994). The ETS domain protein pointed-P2 is a target of MAP kinase in the sevenless signal transduction pathway. *Nature* **370**, 386-389.

Buratti, E., De Conti, L., Stuani, C., Romano, M., Baralle, M. and Baralle, F. (2010). Nuclear factor TDP-43 can affect selected microRNA levels. *Febs Journal* **277**, 2268-2281.

Cao, C., Liu, Y. and Lehmann, M. (2007). Fork head controls the timing and tissue selectivity of steroid-induced developmental cell death. *The Journal of cell biology* **176**, 843-852.

Chang, H. C., Solomon, N. M., Wassarman, D. A., Karim, F. D., Therrien, M., Rubin, G. M. and Wolff, T. (1995). phyllopod functions in the fate determination of a subset of photoreceptors in Drosophila. *Cell* **80**, 463-472.

Chen, X., Fan, Z., McGee, W., Chen, M., Kong, R., Wen, P., Xiao, T., Chen, X., Liu, J. and Zhu, L. (2017). TDP-43 regulates cancer-associated microRNAs. *Protein & Cell*, 1-19.

Coleman, H. A., Labrador, J.-P., Chance, R. K. and Bashaw, G. J. (2010). The Adam family metalloprotease Kuzbanian regulates the cleavage of the roundabout receptor to control axon repulsion at the midline. *Development* **137**, 2417-2426.

Coyne, A. N., Yamada, S. B., Siddegowda, B. B., Estes, P. S., Zaepfel, B. L., Johannesmeyer, J. S., Lockwood, D. B., Pham, L. T., Hart, M. P. and Cassel, J. A. (2015). Fragile X protein mitigates TDP-43 toxicity by remodeling RNA granules and restoring translation. *Human Molecular Genetics* **24**, 6886-6898.

Darzacq, X., Jády, B. E., Verheggen, C., Kiss, A. M., Bertrand, E. and Kiss, T. (2002). Cajal body-specific small nuclear RNAs: a novel class of 2′-O-methylation and pseudouridylation guide RNAs. *The EMBO journal* **21**, 2746-2756.

Deryusheva, S. and Gall, J. G. (2009). Small Cajal body–specific RNAs of Drosophila function in the absence of Cajal bodies. *Molecular biology of the cell* **20**, 5250-5259.

Dieci, G., Preti, M. and Montanini, B. (2009). Eukaryotic snoRNAs: a paradigm for gene expression flexibility. *Genomics* **94**, 83-88.

Dragon, F., Lemay, V. and Trahan, C. (2006). snoRNAs: Biogenesis, Structure and Function. *eLS*.

Dupuis-Sandoval, F., Poirier, M. and Scott, M. S. (2015). The emerging landscape of small nucleolar RNAs in cell biology. *WIREs RNA* **6**, 381-397.

Edwards, T. N. and Meinertzhagen, I. A. (2009). Photoreceptor neurons find new synaptic targets when misdirected by overexpressing runt in Drosophila. *Journal of Neuroscience* **29**, 828-841.

Enomoto, M., Vaughen, J. and Igaki, T. (2015). Non-autonomous overgrowth by oncogenic niche cells: Cellular cooperation and competition in tumorigenesis. *Cancer science* **106**, 1651-1658.

Falaleeva, M. and Stamm, S. (2013). Processing of snoRNAs as a new source of regulatory non-coding RNAs. *Bioessays* **35**, 46-54.

Fernández-Medarde, A. and Santos, E. (2011). Ras in cancer and developmental diseases. *Genes & cancer* **2**, 344-358.

Frankfort, B. J. and Mardon, G. (2002). R8 development in the Drosophila eye: a paradigm for neural selection and differentiation. *Development* **129**, 1295-1306.

Freeman, A., Bowers, M., Mortimer, A. V., Timmerman, C., Roux, S., Ramaswami, M. and Sanyal, S. (2010). A new genetic model of activity-induced Ras signaling dependent pre-synaptic plasticity in Drosophila. *Brain research* **1326**, 15-29.

Friedman, A. A., Tucker, G., Singh, R., Yan, D., Vinayagam, A., Hu, Y., Binari, R., Hong, P., Sun, X. and Porto, M. (2011). Proteomic and functional genomic landscape of receptor tyrosine kinase and ras to extracellular signal–regulated kinase signaling. *Science signaling* **4**, rs10.

Geisler, S. and Coller, J. (2013). RNA in unexpected places: long non-coding RNA functions in diverse cellular contexts. *Nature reviews Molecular cell biology* **14**, 699-712.

Goldstein, I., Rainy, N., Rechavi, O. and Kloog, Y. (2014). Intercellular transfer of Ras: Implications for immunity. Taylor & Francis.

Henras, A. K., Plisson-Chastang, C., O'Donohue, M. F., Chakraborty, A. and Gleizes, P. E. (2015). An overview of pre-ribosomal RNA processing in eukaryotes. *Wiley Interdisciplinary Reviews: RNA* **6**, 225-242.

Honda, D., Ishigaki, S., Iguchi, Y., Fujioka, Y., Udagawa, T., Masuda, A., Ohno, K., Katsuno, M. and Sobue, G. (2014). The ALS/FTLD-related RNA-binding proteins TDP-43 and FUS have common downstream RNA targets in cortical neurons. *FEBS Open Bio* **4**, 1-10.

Huang, A. M. and Rubin, G. M. (2000). A misexpression screen identifies genes that can modulate RAS1 pathway signaling in Drosophila melanogaster. *Genetics* **156**, 1219-1230.

Huang, D. W., Sherman, B. T., Zheng, X., Yang, J., Imamichi, T., Stephens, R. and Lempicki, R. A. (2009). Extracting biological meaning from large gene lists with DAVID. *Current protocols in bioinformatics*, 13.11. 11-13.11. 13.

Huang, Y., Zhang, J. L., Yu, X. L., Xu, T. S., Wang, Z. B. and Cheng, X. C. (2013). Molecular functions of small regulatory noncoding RNA. *Biochemistry (Moscow)* **78**, 221-230.

Jékely, G., Sung, H.-H., Luque, C. M. and Rørth, P. (2005). Regulators of endocytosis maintain localized receptor tyrosine kinase signaling in guided migration. *Developmental cell* **9**, 197-207.

Jiang, H., Wang, Y., Ai, M., Wang, H., Duan, Z., Wang, H., Zhao, L., Yu, J., Ding, Y. and Wang, S. (2017). Long noncoding RNA CRNDE stabilized by hnRNPUL2 accelerates cell proliferation and migration in colorectal carcinoma via activating Ras/MAPK signaling pathways. *Cell death & disease* **8**, e2862.

Jinesh, G., Sambandam, V., Vijayaraghavan, S., Balaji, K. and Mukherjee, S. (2018). Molecular genetics and cellular events of K-Ras-driven tumorigenesis. *Oncogene* **37**, 839.

Johnson, S. M., Grosshans, H., Shingara, J., Byrom, M., Jarvis, R., Cheng, A., Labourier, E., Reinert, K. L., Brown, D. and Slack, F. J. (2005). RAS is regulated by the let-7 microRNA family. *Cell* **120**, 635-647.

Johnson, T. K., Cockerell, F. E. and McKechnie, S. W. (2011). Transcripts from the Drosophila heat-shock gene hsr-omega influence rates of protein synthesis but hardly affect resistance to heat knockdown. *Molecular genetics and genomics* **285**, 313-323.

Jose, A. M. (2015). Movement of regulatory RNA between animal cells. *genesis* **53**, 395-416.

Karim, F. D., Chang, H. C., Themen, M., Wassarman, D. A., Laverty, T. and Rubin, G. M. (1996). A screen for genes that function downstream of Ras1 during Drosophila eye development. *Genetics* **143**, 315-329.

Karim, F. D. and Rubin, G. M. (1998). Ectopic expression of activated Ras1 induces hyperplastic growth and increased cell death in Drosophila imaginal tissues. *Development* **125**, 1-9.

Karin, M. and Hunter, T. (1995). Transcriptional control by protein phosphorylation: signal transmission from the cell surface to the nucleus. *Current Biology* **5**, 747-757.

Katsushima, K., Natsume, A., Ohka, F., Shinjo, K., Hatanaka, A., Ichimura, N., Sato, S., Takahashi, S., Kimura, H. and Totoki, Y. (2016). Targeting the Notch-regulated non-coding RNA TUG1 for glioma treatment. *Nature communications* **7**, 13616.

Kimmel, B. E., Heberlein, U. and Rubin, G. M. (1990). The homeo domain protein rough is expressed in a subset of cells in the developing Drosophila eye where it can specify photoreceptor cell subtype. *Genes & Development* **4**, 712-727.

Kiss, A. M., Jády, B. E., Darzacq, X., Verheggen, C., Bertrand, E. and Kiss, T. (2002). A Cajal body-specific pseudouridylation guide RNA is composed of two box H/ACA snoRNA-like domains. *Nucleic acids research* **30**, 4643-4649.

Kiss, T. (2004). Biogenesis of small nuclear RNPs. *Journal of cell science* **117**, 5949-5951.

Komura-Kawa, T., Hirota, K., Shimada-Niwa, Y., Yamauchi, R., Shimell, M., Shinoda, T., Fukamizu, A., O'Connor, M. B. and Niwa, R. (2015). The Drosophila zinc finger transcription factor Ouija board controls ecdysteroid biosynthesis through specific regulation of spookier. *PLoS Genet* **11**, e1005712.

Kosman, D., Small, S. and Reinitz, J. (1998). Rapid preparation of a panel of polyclonal antibodies to Drosophila segmentation proteins. *Development genes and evolution* **208**, 290-294.

Kotake, Y., Naemura, M., Kitagawa, K., Niida, H., Tsunoda, T., Shirasawa, S. and Kitagawa, M. (2016). Oncogenic Ras influences the expression of multiple lncRNAs. *Cytotechnology* **68**, 1591-1596.

Kramer, S., West, S. R. and Hiromi, Y. (1995). Cell fate control in the Drosophila retina by the orphan receptor seven-up: its role in the decisions mediated by the ras signaling pathway. *Development* **121**, 1361-1372.

Kumar, J. P. and Moses, K. (2000). Cell fate specification in the Drosophila retina. In *Vertebrate Eye Development*, pp. 93-114: Springer.

Kumar, L., Haque, R. and Nazir, A. (2016). Role of microRNA Let-7 in modulating multifactorial aspect of neurodegenerative diseases: An overview. *Molecular neurobiology* **53**, 2787-2793.

Lakhotia, S. C. (2011). Forty years of the 93D puff of Drosophila melanogaster. *J. Biosciences* **36**, 399-423.

---- (2012). Long non-coding RNAs coordinate cellular responses to stress. *WIREs RNA* **3**, 779-796.

---- (2016). Non-coding RNAs have key roles in cell regulation. *Proc. Indian Natn. Sci. Acad.* **82**, in press.

Lakhotia, S. C. (2017a). From heterochromatin to long noncoding RNAs in Drosophila: Expanding the arena of gene function and regulation. In *Long Non Coding RNA Biology* (ed. M. R. S. Rao), pp. 75-118. Singapore: Springer Nature Singapore Pte Ltd.

Lakhotia, S. C. (2017b). Non-coding RNAs demystify constitutive heterochromatin as essential modulator of epigenotype. *The Nucleus* **60**, 299-314.

Lakhotia, S. C., Mallik, M., Singh, A. K. and Ray, M. (2012). The large noncoding hsrω-n transcripts are essential for thermotolerance and remobilization of hnRNPs, HP1 and RNA polymerase II during recovery from heat shock in Drosophila. *Chromosoma* **121**, 49-70.

Lee, J. H., Cho, K. S., Lee, J., Kim, D., Lee, S.-B., Yoo, J., Cha, G.-H. and Chung, J. (2002). Drosophila PDZ-GEF, a guanine nucleotide exchange factor for Rap1 GTPase, reveals a novel upstream regulatory mechanism in the mitogen-activated protein kinase signaling pathway. *Molecular and cellular biology* **22**, 7658-7666.

Liang, X., Mahato, S., Hemmerich, C. and Zelhof, A. C. (2016). Two temporal functions of Glass: Ommatidium patterning and photoreceptor differentiation. *Developmental biology* **414**, 4-20.

Liao, G.-c., Rehm, E. J. and Rubin, G. M. (2000). Insertion site preferences of the P transposable element in Drosophila melanogaster. *Proceedings of the National Academy of Sciences* **97**, 3347-3351.

Liu, B., Sun, L., Liu, Q., Gong, C., Yao, Y., Lv, X., Lin, L., Yao, H., Su, F. and Li, D. (2015). A cytoplasmic NF-κB interacting long noncoding RNA blocks IκB phosphorylation and suppresses breast cancer metastasis. *Cancer cell* **27**, 370-381.

Machamer, J. B., Woolums, B. M., Fuller, G. G. and Lloyd, T. E. (2018). FUS causes synaptic hyperexcitability in Drosophila dendritic arborization neurons. *Brain Research* **1693**, 55-66.

Mallik, M. and Lakhotia, S. (2009). RNAi for the large non-coding hsr omega transcripts suppresses polyglutamine pathogenesis in *Drosophila* models. *Rna Biology* **6**, 464-478.

---- (2010). Improved Activities of CREB Binding Protein, Heterogeneous Nuclear Ribonucleoproteins and Proteasome Following Downregulation of Noncoding hsr omega Transcripts Help Suppress Poly(Q) Pathogenesis in Fly Models. *Genetics* **184**, 927-945.

Mallik, M. and Lakhotia, S. C. (2011). Pleiotropic consequences of misexpression of the developmentally active and stress-inducible non-coding *hsr omega* gene in *Drosophila*. *J. Biosciences* **36**, 265-280.

Mattick, J. and Makunin, I. (2006). Non-coding RNA. *Human molecular genetics* **15 Spec No 1**, 29.

Mavromatakis, Y. E. and Tomlinson, A. (2016). R7 Photoreceptor Specification in the Developing Drosophila Eye: The Role of the Transcription Factor Deadpan. *PLoS genetics* **12**, e1006159.

McMahon, M., Contreras, A. and Ruggero, D. (2015). Small RNAs with big implications: new insights into H/ACA snoRNA function and their role in human disease. *Wiley Interdisciplinary Reviews: RNA* **6**, 173-189.

Metsalu, T. and Vilo, J. (2015). ClustVis: a web tool for visualizing clustering of multivariate data using Principal Component Analysis and heatmap. *Nucleic acids research* **43**, W566-W570.

Misawa, A., Takayama, K. i., Fujimura, T., Homma, Y., Suzuki, Y. and Inoue, S. (2017). Androgen-induced lncRNA POTEF-AS1 regulates apoptosis-related pathway to facilitate cell survival in prostate cancer cells. *Cancer science* **108**, 373-379.

Mondal, K., VijayRaghavan, K. and Varadarajan, R. (2007). Design and utility of temperature-sensitive Gal4 mutants for conditional gene expression in Drosophila. *Fly* **1**, 282-286.

Morris, K. V. and Mattick, J. S. (2014). The rise of regulatory RNA. *Nature Reviews Genetics* **15**, 423-437.

Moses, K., Ellis, M. C. and Rubin, G. M. (1989). The glass gene encodes a zinc-finger protein required by Drosophila photoreceptor cells. *Nature* **340**, 531.

Moss, E. G. and Tang, L. (2003). Conservation of the heterochronic regulator Lin-28, its developmental expression and microRNA complementary sites. *Developmental biology* **258**, 432-442.

Newman, M. A., Thomson, J. M. and Hammond, S. M. (2008). Lin-28 interaction with the Let-7 precursor loop mediates regulated microRNA processing. *Rna* **14**, 1539-1549.

O'Neill, E. M., Rebay, I., Tjian, R. and Rubin, G. M. (1994). The activities of two Ets-related transcription factors required for Drosophila eye development are modulated by the Ras/MAPK pathway. *Cell* **78**, 137-147.

Olivier, J. P., Raabe, T., Henkemeyer, M., Dickson, B., Mbamalu, G., Margolis, B., Schlessinger, J., Hafen, E. and Pawson, T. (1993). A Drosophila SH2-SH3 adaptor protein implicated in coupling

the sevenless tyrosine kinase to an activator of Ras guanine nucleotide exchange, Sos. *Cell* **73**, 179-191.

Onorati, M. C., Lazzaro, S., Mallik, M., Ingrassia, A. M., Carreca, A. P., Singh, A. K., Chaturvedi, D. P., Lakhotia, S. C. and Corona, D. F. (2011). The ISWI chromatin remodeler organizes the hsromega ncRNA-containing omega speckle nuclear compartments. *PLoS Genet* **7**, e1002096.

Parry, J. M. and Sundaram, M. V. (2014). A non-cell-autonomous role for Ras signaling in C. elegans neuroblast delamination. *Development* **141**, 4279-4284.

Peng, W., Koirala, P. and Mo, Y. (2017). LncRNA-mediated regulation of cell signaling in cancer. *Oncogene*.

Piccolo, L. L., Bonaccorso, R., Attardi, A., Li Greci, L., Romano, G., Sollazzo, M., Giurato, G., Ingrassia, A. M. R., Feiguin, F. and Corona, D. F. (2018). Loss of ISWI Function in Drosophila Nuclear Bodies Drives Cytoplasmic Redistribution of Drosophila TDP-43. *Int. J. Mol. Sci.* **19**, 1082.

Piccolo, L. L. and Yamaguchi, M. (2017). RNAi of arcRNA hsrω affects sub-cellular localization of Drosophila FUS to drive neurodiseases. *Experimental Neurology* **292**, 125-134.

Pickup, A. T., Lamka, M. L., Sun, Q., Yip, M. L. R. and Lipshitz, H. D. (2002). Control of photoreceptor cell morphology, planar polarity and epithelial integrity during Drosophila eye development. *Development* **129**, 2247-2258.

Prasanth, K., Rajendra, T., Lal, A. and Lakhotia, S. (2000). Omega speckles-a novel class of nuclear speckles containing hnRNPs associated with noncoding hsr-omega RNA in Drosophila. *Journal of cell science* **113**, 3485-3497.

Prober, D. A. and Edgar, B. A. (2000). Ras1 promotes cellular growth in the Drosophila wing. *Cell* **100**, 435-446.

Pylayeva-Gupta, Y., Grabocka, E. and Bar-Sagi, D. (2011). RAS oncogenes: weaving a tumorigenic web. *Nature Reviews Cancer* **11**, 761-774.

Ray, M. and Lakhotia, S. C. (2015). The commonly used eye-specific sev-GAL4 and GMR-GAL4 drivers in Drosophila melanogaster are expressed in tissues other than eyes also. *J. Genetics* **94**, 407-416.

Ray, M. and Lakhotia, S. C. (2017). Altered hsrω lncRNA levels in activated Ras background further enhance Ras activity in Drosophila eye and induces more R7 photoreceptors. *bioRxiv*, DOI: 10.1101/224543.

Ray, P. and Lakhotia, S. C. (1998). Interaction of the non-protein-coding developmental and stress-inducible hsrω gene with Ras genes of *Drosophila melanogaster*. *J. Biosciences* **23**, 377-386.

Rhee, D. Y., Cho, D.-Y., Zhai, B., Slattery, M., Ma, L., Mintseris, J., Wong, C. Y., White, K. P., Celniker, S. E. and Przytycka, T. M. (2014). Transcription factor networks in Drosophila melanogaster. *Cell reports* **8**, 2031-2043.

Richard, P., Darzacq, X., Bertrand, E., Jády, B. E., Verheggen, C. and Kiss, T. (2003). A common sequence motif determines the Cajal body-specific localization of box H/ACA scaRNAs. *The EMBO journal* **22**, 4283-4293.

Romano, M., Buratti, E., Romano, G., Klima, R., Belluz, L. D. B., Stuani, C., Baralle, F. and Feiguin, F. (2014). Evolutionarily conserved heterogeneous nuclear ribonucleoprotein (hnRNP) A/B proteins functionally interact with human and Drosophila TAR DNA-binding protein 43 (TDP-43). *J. Biol. Chem.* **289**, 7121-7130.

Rotblat, B., Leprivier, G. and Sorensen, P. (2011). A possible role for long non-coding RNA in modulating signaling pathways. *Medical hypotheses* **77**, 962-965.

Sieglitz, F., Matzat, T., Yuva-Aydemir, Y., Neuert, H., Altenhein, B. and Klämbt, C. (2013). Antagonistic feedback loops involving Rau and Sprouty in the Drosophila eye control neuronal and glial differentiation. *Sci. Signal.* **6**, ra96-ra96.

Singh, A. K. and Lakhotia, S. C. (2015). Dynamics of hnRNPs and omega speckles in normal and heat shocked live cell nuclei of *Drosophila melanogaster*. *Chromosoma* **124**, 367-383.

Siprashvili, Z., Webster, D. E., Johnston, D., Shenoy, R. M., Ungewickell, A. J., Bhaduri, A., Flockhart, R., Zarnegar, B. J., Che, Y. and Meschi, F. (2016). The noncoding RNAs SNORD50A and SNORD50B bind K-Ras and are recurrently deleted in human cancer. *Nature genetics* **48**, 53-58.

Sloan, K. E., Warda, A. S., Sharma, S., Entian, K.-D., Lafontaine, D. L. and Bohnsack, M. T. (2017). Tuning the ribosome: the influence of rRNA modification on eukaryotic ribosome biogenesis and function. *RNA biology*, 1-16.

Sotillos, S., Roch, F. and Campuzano, S. (1997). The metalloprotease-disintegrin Kuzbanian participates in Notch activation during growth and patterning of Drosophila imaginal discs. *Development* **124**, 4769-4779.

Stratoulias, V., Heino, T. I. and Michon, F. (2014). Lin-28 regulates oogenesis and muscle formation in Drosophila melanogaster. *PLoS One* **9**, e101141.

Takino, K., Ohsawa, S. and Igaki, T. (2014). Loss of Rab5 drives non-autonomous cell proliferation through TNF and Ras signaling in Drosophila. *Developmental biology* **395**, 19-28.

Tomlinson, A., Mavromatakis, Y. E. and Struhl, G. (2011). Three distinct roles for notch in Drosophila R7 photoreceptor specification. *PLoS biology* **9**, e1001132.

Tomlinson, A. and Struhl, G. (2001). Delta/Notch and Boss/Sevenless signals act combinatorially to specify the Drosophila R7 photoreceptor. *Molecular cell* **7**, 487-495.

Trapnell, C., Roberts, A., Goff, L., Pertea, G., Kim, D., Kelley, D. R., Pimentel, H., Salzberg, S. L., Rinn, J. L. and Pachter, L. (2012). Differential gene and transcript expression analysis of RNA-seq experiments with TopHat and Cufflinks. *Nature protocols* **7**, 562-578.

Udolph, G., Rath, P., Tio, M., Toh, J., Fang, W., Pandey, R., Technau, G. M. and Chia, W. (2009). On the roles of Notch, Delta, kuzbanian, and inscuteable during the development of Drosophila embryonic neuroblast lineages. *Developmental biology* **336**, 156-168.

Uhlirova, M., Jasper, H. and Bohmann, D. (2005). Non-cell-autonomous induction of tissue overgrowth by JNK/Ras cooperation in a Drosophila tumor model. *Proceedings of the National Academy of Sciences of the United States of America* **102**, 13123-13128.

Viswanathan, S. R., Daley, G. Q. and Gregory, R. I. (2008). Selective blockade of microRNA processing by Lin28. *Science* **320**, 97-100.

Wang, X.-R., Luo, H., Li, H.-L., Cao, L., Wang, X.-F., Yan, W., Wang, Y.-Y., Zhang, J.-X., Jiang, T. and Kang, C.-S. (2013). Overexpressed let-7a inhibits glioma cell malignancy by directly targeting K-ras, independently of PTEN. *Neuro-oncology* **15**, 1491-1501.

Wang, Y., Wang, Y., Li, J., Zhang, Y., Yin, H. and Han, B. (2015). CRNDE, a long-noncoding RNA, promotes glioma cell growth and invasion through mTOR signaling. *Cancer letters* **367**, 122-128.

Yan, D. and Perrimon, N. (2015). spenito is required for sex determination in Drosophila melanogaster. *Proceedings of the National Academy of Sciences* **112**, 11606-11611.

Yan, H., Chin, M.-L., Horvath, E. A., Kane, E. A. and Pfleger, C. M. (2009). Impairment of ubiquitylation by mutation in Drosophila E1 promotes both cell-autonomous and non-cell-autonomous Ras-ERK activation in vivo. *J Cell Sci* **122**, 1461-1470.

Yang, Y., Xu, S., Xia, L., Wang, J., Wen, S., Jin, P. and Chen, D. (2009). The bantam microRNA is associated with drosophila fragile X mental retardation protein and regulates the fate of germline stem cells. *PLoS genetics* **5**.

Zhang, D., Zhang, G., Hu, X., Wu, L., Feng, Y., He, S., Zhang, Y., Hu, Z., Yang, L. and Tian, T. (2017a). Oncogenic RAS regulates long non-coding RNA Orilnc1 in human cancer. *Cancer Research*, canres. 1768.2016.

---- (2017b). Oncogenic RAS Regulates Long Noncoding RNA Orilnc1 in Human Cancer. *Cancer research* **77**, 3745-3757.

Zhu, M. Y., Wilson, R. and Leptin, M. (2005). A screen for genes that influence fibroblast growth factor signal transduction in Drosophila. *Genetics* **170**, 767-777.